

Accepted Manuscript

Design, synthesis and biological evaluation of *N*-phenylquinazolin-4-amine hybrids as dual inhibitors of VEGFR-2 and HDAC

Fan-Wei Peng, Ji Xuan, Ting-Ting Wu, Jia-Yu Xue, Zi-Wei Ren, Da-Ke Liu, Xiu-Qi Wang, Xin-Hang Chen, Jia-Wei Zhang, Yun-Gen Xu, Lei Shi



PII: S0223-5234(15)30419-0

DOI: [10.1016/j.ejmech.2015.12.033](https://doi.org/10.1016/j.ejmech.2015.12.033)

Reference: EJMECH 8273

To appear in: *European Journal of Medicinal Chemistry*

Received Date: 12 June 2015

Revised Date: 14 December 2015

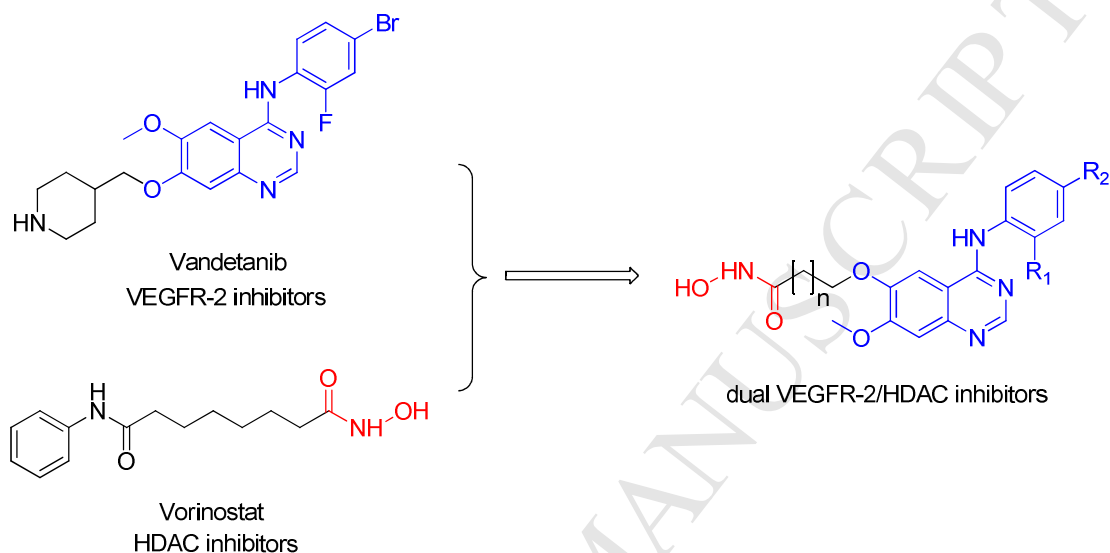
Accepted Date: 16 December 2015

Please cite this article as: F.-W. Peng, J. Xuan, T.-T. Wu, J.-Y. Xue, Z.-W. Ren, D.-K. Liu, X.-Q. Wang, X.-H. Chen, J.-W. Zhang, Y.-G. Xu, L. Shi, Design, synthesis and biological evaluation of *N*-phenylquinazolin-4-amine hybrids as dual inhibitors of VEGFR-2 and HDAC, *European Journal of Medicinal Chemistry* (2016), doi: 10.1016/j.ejmech.2015.12.033.

This is a PDF file of an unedited manuscript that has been accepted for publication. As a service to our customers we are providing this early version of the manuscript. The manuscript will undergo copyediting, typesetting, and review of the resulting proof before it is published in its final form. Please note that during the production process errors may be discovered which could affect the content, and all legal disclaimers that apply to the journal pertain.

Design, synthesis and biological evaluation of *N*-phenylquinazolin-4-amine hybrids as dual inhibitors of VEGFR-2 and HDAC

Fan-Wei Peng^{1†}, Ji Xuan^{3†}, Ting-Ting Wu¹, Jia-Yu Xue², Zi-Wei Ren¹, Da-Ke Liu¹,
Xiu-Qi Wang¹, Xin-Hang Chen¹, Jia-Wei Zhang¹, Yun-Gen Xu^{1*}, Lei Shi^{1*}



A series of hybrids bearing *N*-phenylquinazolin-4-amine and hydroxamic acid moieties were designed, synthesized, and discovered as dual VEGFR-2/HDAC inhibitors.

*Corresponding author. *E-mail address*: xyg@cpu.edu.cn (Y.-G. Xu), shilei@cpu.edu.cn (L. Shi).

†Both authors contributed equally to the work.

Design, synthesis and biological evaluation of *N*-phenylquinazolin-4-amine hybrids as dual inhibitors of VEGFR-2 and HDAC

Fan-Wei Peng^{1†}, Ji Xuan^{3†}, Ting-Ting Wu¹, Jia-Yu Xue², Zi-Wei Ren¹, Da-Ke Liu¹,
Xiu-Qi Wang¹, Xin-Hang Chen¹, Jia-Wei Zhang¹, Yun-Gen Xu^{1*}, Lei Shi^{1*}

1. Jiangsu Key Laboratory of Drug Design and Optimization, Department of Medicinal Chemistry, China Pharmaceutical University, Nanjing 210009, P. R. China
2. Jiangsu Provincial Key Laboratory for Plant Ex Situ Conservation, Institute of Botany, Jiangsu Province and Chinese Academy of Sciences, Nanjing 210014, P. R. China
3. 81 Hospital of PLA, Nanjing 210002, P. R. China

Abstract:

A single agent that simultaneously inhibits multiple targets may offer greater therapeutic benefits in cancer than single-acting agents through interference with multiple pathways and potential synergistic action. In this work, a series of hybrids bearing *N*-phenylquinazolin-4-amine and hydroxamic acid moieties were designed and identified as dual VEGFR-2/HDAC inhibitors. Compound **6fd** exhibited the most potent inhibitory activity against HDAC with IC₅₀ of 2.2 nM and strong inhibitory effect against VEGFR-2 with IC₅₀ of 74 nM. It also showed the most potent inhibitory activity against a human breast cancer cell line MCF-7 with IC₅₀ of 0.85 μM. Docking simulation supported the initial pharmacophoric hypothesis and suggested a common mode of interaction at the active binding sites of VEGFR-2 and HDLP ((Histone Deacetylase-Like Protein), which demonstrates that compound **6fd** is a potential agent for cancer therapy deserving further researching.

Keywords: *N*-phenylquinazolin-4-amine hybrid, VEGFR-2, HDAC, dual inhibitor

*Corresponding author. *E-mail address*: xyg@cpu.edu.cn (Y.-G. Xu), shilei@cpu.edu.cn (L. Shi).

†Both authors contributed equally to the work.

1. Introduction

Angiogenesis, the process of new blood vessels formation from existing vasculature, is a normal physiological event for organ development. It occurs during tissue growth from embryonic development through to maturity. It is also activated during wound repairment and certain stages of menstrual cycle [1,2]. However, abnormal regulation of angiogenesis has been involved in the development of various diseases such as rheumatoid arthritis, psoriasis, diabetic retinopathy, tumor growth, and tumor metastasis [2-7]. Among the angiogenic factors identified to date, vascular endothelial growth factor (VEGF) and its receptor tyrosine kinase VEGFR-2 or kinase insert domain receptor (KDR) are the most important regulator of tumor angiogenesis [8,9]. It is well demonstrated that upon binding its ligand, VEGFR-2 undergoes receptor dimerization and autophosphorylation and initiates downstream signaling, ultimately leading to tumor angiogenesis, vascular permeability enhancement, proliferation, and migration [10,11]. Consequently, inhibition of the VEGF/VEGFR-2 signaling pathway has become a valuable approach in the treatment of cancers. Indeed, a number of angiogenesis inhibitors of VEGFR-2 have been approved by FDA or effectively demonstrated in preclinical and clinical settings. Bevacizumab, a monoclonal antibody to VEGF, has been approved by the FDA for the treatment of non-small-cell lung cancer [12] and metastatic colorectal cancer [13]. Ramucirumab, a mAb antibody (human IgG1) directed against VEGFR-2, has been approved by FDA in 2014 for advanced gastric or gastro-esophageal junction adenocarcinoma and metastatic non-small-cell lung carcinoma [14]. In addition, small-molecule tyrosine kinase inhibitors of VEGFR-2, such as Sunitinib [15], Sorafenib [16], and Vandetanib [17] have been approved for treatment of various types of cancers including renal cell carcinoma, gastrointestinal stromal tumor (GIST), hepatocellular carcinoma, thyroid cancer, and soft tissue sarcom.

However, a significant number of patients do not respond to VEGFR-2 targeted therapy. Furthermore, the effectiveness of these angiogenesis inhibitors is also limited by the drug resistance that frequently emerges following treatment [18-20]. To

overcome the low response rate and acquired drug resistance to tyrosine kinase inhibitors (TKIs), a number of strategies have been tested, including combination therapies and development of multi-targeted inhibitors [21,22].

Histone deacetylases (HDACs) are a class of enzymes that catalyze the removal of acetyl groups from the ϵ -amino groups of lysine residues present within the N-terminal extension of the core histones, leading to chromatin condensation and transcriptional repression [23,24]. In addition to regulating the acetylation state of histones, HDACs can bind to, deacetylate and regulate the activity of a number of non-histone proteins, including transcription factors such as p53, E2F1, and NF- κ B and proteins with diverse biological functions such as α -tubulin, Ku70 and Hsp90 [24]. Eighteen HDACs have been identified in humans, and they are subdivided into four structurally and functionally different phylogenetic classes. Among them, Class I HDACs (1, 2, 3, and 8) and Class II HDACs (4, 5, 6, 7, 9, and 10) are zinc dependent proteases [25]. It has been widely recognized that zinc-containing HDACs are promising targets for therapeutic interventions intended to reverse aberrant epigenetic states associated with cancer [26-28]. Consequently, considerable effort has been devoted to develop HDAC inhibitors recently [29-34].

HDAC inhibitors have been demonstrated to synergize with other antitumor agents, including RTK inhibitors, to suppress proliferation and induce apoptosis in tumor cells, even to overcome TKI resistance [35-39]. Recently, multi-acting inhibitors against HDAC and RTK have been reported [40-44]. But the report of VEGFR-2/HDAC dual inhibitors is rare [45]. In this study, a series of *N*-phenylquinazolin-4-amine hybrids were rationally designed and synthesized as dual VEGFR-2/HDAC inhibitors by combination of pharmacophores of two reference drugs, Vandetanib and Vorinostat, which were used to achieve VEGFR-2 and HDAC inhibition, respectively (Figure 1).

2. Results and discussion

2.1. Chemistry

The synthetic route to obtain the desired target compounds is outlined in Scheme

1 according to the literature with some modifications [40]. Compounds **3a-3f** were prepared through the coupling of substituted anilines with 4-chloro-7-methoxyquinazolin-6-yl acetate (**2**), which was prepared through chlorination of 7-methoxy-4-oxo-3,4-dihydroquinazolin-6-yl acetate (**1**). Hydrolysis of the acetyl group on compounds **3a-3f** using lithium hydroxide gave corresponding phenol intermediates **4a-4f**. Alkylation of the phenolic hydroxyl group on compounds **4a-4f** with various chain lengths of ethyl bromoalkanoate gave ethyl ester intermediates **5aa-5fd**. Conversion of ethyl esters **5aa-5fd** to hydroxamic acids using freshly prepared hydroxylamine furnished target *N*-phenylquinazolin-4-amine hybrids **6aa-6fd**.

2.2. Biological evaluation

The *in vitro* enzymatic inhibitory activities of the target compounds against VEGFR-2 and HDAC were evaluated. Additionally, the *in vitro* antiproliferative effects of the targeted compounds against MCF-7, a human breast adenocarcinoma cell line, were also tested. The results were summarized in Table 1.

2.2.1. VEGFR-2 inhibition

As shown in Table 1, the target compounds **6aa-6fd** exhibited mild to moderate VEGFR-2 inhibitory activities compared to the reference compound Vandetanib. Among them, compounds **6fa-6fd** with *para*-bromo substituent on the phenyl ring exhibited potent inhibitory activity against VEGFR-2 kinase with IC₅₀ values ranging from 74 nM to 153 nM, which was comparable to the positive drug Vandetanib (IC₅₀ = 54 nM). Among them, compound **6fb** exhibited the most potent VEGFR-2 inhibitory activity with IC₅₀ of 59 nM. It seems that the change of the length of carbon chain (n = 2 to 5) does not influence VEGFR-2 inhibition significantly. On the contrary, the type and position of halogen substituent on the phenyl ring play important roles in the VEGFR-2 inhibition. Compared with compounds **6fa-6fd**, the inhibitory activity of compounds **6ea-6ed** with *ortho*-bromo substituent decreased dramatically with IC₅₀ over 10000 nM against VEGFR-2. It is likely that *ortho*-Br

restricts the free rotation of the benzene ring. This is supported by the fact that the rank order of the VEGFR-2 inhibitory activity is *ortho*-Br < *ortho*-Cl <= *ortho*-F < *ortho*-H. Compounds **6ba-6bd** with *para*-fluoro substituent showed stronger inhibitory activity against VEGFR-2 (IC₅₀ ranged from 270 nM to 524 nM) than compounds **6aa-6ad** with *ortho*-fluoro substituent (IC₅₀ ranged from 754 nM to 918 nM). Similarly, compounds **6cd-6dd** with *para*-chloro substituent showed weaker inhibition against VEGFR-2 (IC₅₀ ranged from 364 nM to 857 nM) than compounds **6da-6dd** with *ortho*-fluoro substituent (IC₅₀ ranged from 182 nM to 313 nM). All the above results indicated that introduction of bromo substituent at *para* position on the phenyl ring is favorable for the VEGFR-2 inhibition. It is worth noting that 7-(4-(3-ethynylphenylamino)-7-methoxyquinazolin-6-ylloxy)-N-hydroxyheptanamide (CUDC-101) reported by Cai et.al. exhibited potent inhibitory activities against HDAC, EGFR, and HER2 but weak inhibitory activity against VEGFR-2 [40]. The main difference between our synthesized compounds and CUDC-101 is the substituent and its position on the phenyl ring. The substituent on the phenyl ring of CUDC-101 is *meta*-ethynyl group while of our synthesized compounds is *para*- or *ortho*- substituted halogen.

2.2.2. HDAC inhibition

Data in Table 1 illustrated that the target compounds **6aa-6fd** exhibited moderate to potent HDAC inhibitory activities, which suggested that the *N*-phenylquinazolin-4-amine moiety of the target compounds is a suitable cap group for HDAC inhibitor. Among the compounds tested, compound **6fd** exhibited the most potent HDAC inhibitory activity with IC₅₀ of 2.2 nM, which was 7-fold higher than the reference compound Vorinostat (IC₅₀ = 15 nM). Obviously, increasing the length of the hydroxamic acid side chain increases HDAC inhibitory activity by comparing the HDAC inhibitory activity of compounds **6fa-6fd** with the same substituent (*para*-bromo) on the phenyl ring. The shortest chain hybrid **6fa** (n = 2) showed the weakest HDAC inhibitory activity with IC₅₀ of 545 nM. Moderate HDAC inhibition was observed when the carbon chain length between the quinazoline C6 oxygen and

the hydroxamic acid carbonyl group reached 4 carbons ($n = 3$, compound **6fb**, $IC_{50} = 68$ nM). The HDAC inhibitory activity further increased with the carbon chain length of 5 carbons ($n=4$, compound **6fc**, $IC_{50} = 68$ nM). The optimal carbon chain length is 6 carbons ($n = 5$, compound **6fd**, $IC_{50} = 2.2$ nM). This discipline was also found in other *para* or *ortho* halogen substituted hybrids. In addition, halogen substituent on the phenyl ring affects the HDAC inhibitory to some extent. The inhibitory activities against HDAC of compounds **6bd**, **6dd** and **6fd** with different *para*-halogen substituents increased in the following order: fluoro substituted compound **6bd**, ($IC_{50} = 8.5$ nM) < chloro substituted compound **6bd** ($IC_{50} = 3.2$ nM) < bromo substituted compound **6bd** ($IC_{50} = 2.2$ nM). This rule was also found in other *para* or *ortho* halogen substituted compounds with the same carbon chain length. Besides, the position of halogen substituent has certain impact on HDAC inhibition. In general, compounds with halogen substituent at *para* position on the phenyl ring showed more potent activity against HDAC than compounds with the same carbon chain length and the same halogen substituent at *ortho* position.

In order to further investigate the HDAC isoforms selectivity, compound **6fd** with the most potent HDAC inhibitory activity was chosen to perform enzyme inhibitory assays against a series of HDAC isoenzymes, including HDAC1, HDAC2, HDAC6 and HDAC8. Data in Table 2 indicated that compound **6fd** showed potent inhibitory activities against HDAC1, HDAC2, HDAC6 and HDAC8, with IC_{50} of 1.8 nM, 3.3 nM, 16.4 nM and 4.6 nM, respectively.

2.2.3. Cell growth inhibition

To further explore the antitumor effect of these VEGFR-2/HDAC inhibitors, all the synthesized target compounds **6aa–6fd** were evaluated for their anticancer activities against a human breast cancer cell line MCF-7 by MTT assay. The results were also summarized in Table 1. Among the tested compounds, compound **6fd** with the most potent HDAC inhibitory activity and strong VEGFR-2 inhibitory activity also exhibited the most potent anticancer activities with the IC_{50} value of 0.85 μ M against MCF-7, which showed greater potency than the reference compounds

Vandetanib ($IC_{50} = 18.5 \mu\text{M}$) and Vorinostat ($IC_{50} = 4.2 \mu\text{M}$).

It seemed that the SARs analysis result of antiproliferation activities of the tested compounds were more consistent with their HDAC inhibitory activities. This was probably due to their potent inhibitory activities against HDAC but moderate inhibitory activities against VEGFR-2.

2.3. Molecular docking studies

The possible binding modes of the synthesized target compounds on VEGFR-2 and HDAC were explored with the representative compound **6fd** using the Discovery Studio 3.1/CDOCKER protocol.

Figure 2 demonstrates the compound **6fd** docking into the ATP-binding cavity of VEGFR-2 kinase (PDB code: 2QU5) [46]. In the binding model, the carbonyl oxygen atom of compound **6fd** forms two hydrogen bonds with the amino hydrogen atoms of Asn923 (O...H-N: 2.2 Å). Besides, the terminal hydroxyl hydrogen atom of compound **6fd** forms another hydrogen bond with the carbonyl oxygen atom of Leu840 (O...H-O: 1.9 Å). Both the pyrimidine ring and the phenyl ring of quinazoline moiety form π -cation interactions (distance: 4.6 Å for pyrimidine ring and 5.7 Å for phenyl ring) with the terminal amino cation of Lys868.

The binding model of compound **6fd** into the binding site of HDLP (Histone Deacetylase-Like Protein, PDB code: 1C3S) [47] is depicted in Figure 3. In this binding model, the carbonyl oxygen atom of compound **6fd** forms a hydrogen bond with the phenolic hydroxyl hydrogen atom of Tyr297 (O...H-O: 2.1 Å). In addition, the hydrogen atom of amide group forms a hydrogen bond with the imidazole nitrogen atom of His131 (N...H-N: 2.1 Å). Apart from these, the terminal hydroxyl hydrogen atom forms a hydrogen bond with the carbonyl oxygen atom of Gly129 (O...H-O: 2.2 Å). It is obvious that the *N*-phenylquinazolin moiety at the other end of the aliphatic chain is well tolerated.

The nice binding model of compound **6fd** with VEGFR-2 and HDLP indicates that compound **6fd** could be a potent dual VEGFR-2/HDAC inhibitor.

3. Conclusions

A series of hybrids bearing *N*-phenylquinazolin-4-amine and hydroxamic acid side chain moieties have been designed, synthesized, and evaluated *in vitro* as dual inhibitors against VEGFR-2 and HDAC that displayed great antiproliferation potency against a solid tumor cell line (MCF-7). Compound **6fd** exhibited the most potent inhibitory activity against HDAC with IC₅₀ of 2.2 nM and it showed potent inhibition against VEGFR-2 kinase as well with IC₅₀ of 74 nM. *In vitro* cell growth inhibition assays indicated that compound **6fd** also exhibited the greatest inhibitory activities against a human breast cancer cell line MCF-7 with IC₅₀ of 0.85 μM. Molecular docking of the compound **6fd** into the active binding sites of VEGFR-2 and HDLP was performed and the result suggested that compound **6fd** could bind well with these two sites. The above results demonstrated that compound **6fd** could be a potential anticancer agent and deserved further research.

4. Experimental Section

4.1. Chemistry

All solvents and reagents were commercially available and used without further purification. Melting points (uncorrected) were determined on a RY-1 MP apparatus. ESI-MS spectra were recorded on an Agilent/HP 1100 Series LC/MSD Trap SL Mass spectrometer, and ¹H NMR spectra were recorded on a Bruker AV-300 spectrometer at 25 °C with TMS and solvent signals allotted as internal standards. Chemical shifts were reported in ppm (δ). Elemental analyses were performed on a CHN-O-Rapid instrument.

4.1.1. Preparation of 4-chloro-7-methoxyquinazolin-6-yl acetate (2)

A suspension of 7-methoxy-4-oxo-3,4-dihydroquinazolin-6-yl acetate (**1**) (2.34 g) in SOCl₂ (30 mL) and DMF (0.5 mL) was refluxed for 3h. After that, the mixture was concentrated under reduced pressure to give 4-chloro-7-methoxyquinazolin-6-yl acetate (**2**). Yellow powder, yield: 77%. ¹H-NMR (300 MHz; *d*₆-DMSO): 2.08 (s,

3H); 3.73 (s, 3H); 7.55 (s, 1H); 7.50 (s, 1H); 9.44(s, 1H). MS (ESI⁺) *m/z* 253.6 (M+H)⁺.

4.1.2. General procedure for the preparation of the 7-methoxy-4-(phenylamino)quinazolin-6-yl acetate derivatives 3a-3f

A mixture of 4-chloro-7-methoxyquinazolin-6-yl acetate (**2**, 10 mmol) and appropriate substituted anilines (15 mmol) in isopropanol (80 mL) was stirred at reflux for 4 h. The mixture was cooled to room temperature and the resultant precipitate was collected by filtration and washed with isopropanol. The solid was dried to give compounds **3a-3f**.

4-(2-Fluorophenylamino)-7-methoxyquinazolin-6-yl acetate (**3a**)

White powder, yield: 64%. ¹H-NMR (300 MHz; CDCl₃): 2.11 (s, 3H); 3.69 (s, 3H); 7.27 (s, 1H); 7.42-7.68 (m, 4H); 8.11 (s, 1H); 8.61 (s, 1H). MS (ESI⁺) *m/z* 328.1 (M+H)⁺.

4-(4-Fluorophenylamino)-7-methoxyquinazolin-6-yl acetate (**3b**)

White powder, yield: 64%. ¹H-NMR (300 MHz; CDCl₃): 2.14 (s, 3H); 3.70 (s, 3H); 7.26 (s, 1H); 7.43 (d, *J* = 8.1 Hz, 2H); 7.69 (s, 1H); 8.11 (d, *J* = 8.1 Hz, 2H); 8.61 (s, 1H), 11.18 (s, 1H). MS (ESI⁺) *m/z* 328.1 (M+H)⁺.

4-(2-Chlorophenylamino)-7-methoxyquinazolin-6-yl acetate (**3c**)

White powder, yield: 65%. ¹H-NMR (300 MHz; CDCl₃): 2.13 (s, 3H); 3.70 (s, 3H); 7.25 (s, 1H); 7.43-7.66 (m, 4H); 7.75 (s, 1H); 8.12 (s, 1H); 8.61 (s, 1H), 11.22 (s, 1H). MS (ESI⁺) *m/z* 344.1 (M+H)⁺.

4-(4-Chlorophenylamino)-7-methoxyquinazolin-6-yl acetate (**3d**)

White powder, yield: 65%. ¹H-NMR (300 MHz; CDCl₃): 2.12 (s, 3H); 3.68 (s, 3H); 7.21 (s, 1H); 7.37 (d, *J* = 8.4 Hz, 2H); 7.75 (s, 1H); 8.10 (d, *J* = 8.4 Hz, 2H); 8.59 (s, 1H). MS (ESI⁺) *m/z* 344.1 (M+H)⁺.

4-(2-Bromophenylamino)-7-methoxyquinazolin-6-yl acetate (**3e**)

Yellow powder, yield: 62%. ¹H-NMR (300 MHz; CDCl₃): 2.11 (s, 3H); 3.72 (s, 3H); 7.32 (s, 1H); 7.43-7.56 (m, 3H); 7.75 (s, 1H); 8.14 (d, *J* = 8.4 Hz, 1H); 8.63 (s, 1H); 11.05 (s, 1H). MS (ESI⁺) *m/z* 388.0 (M+H)⁺.

4-(4-Bromophenylamino)-7-methoxyquinazolin-6-yl acetate (3f)

Yellow powder, yield: 63%. ¹H-NMR (300 MHz; CDCl₃): 2.16 (s, 3H); 3.71 (s, 3H); 7.16 (s, 1H); 7.41 (d, *J* = 8.7 Hz, 2H); 7.84 (s, 1H); 8.12 (d, *J* = 8.7 Hz, 2H); 8.60 (s, 1H); 11.27 (s, 1H). MS (ESI⁺) *m/z* 388.0 (M+H)⁺.

4.1.3. General procedure for the preparation of the 7-methoxy-4-(phenylamino)quinazolin-6-ol derivatives 4a-4f

A mixture of 7-methoxy-4-(phenylamino)quinazolin-6-yl acetate derivatives (**3a-3f**, 6 mmol) and LiOH·H₂O (19.8 mmol) in methanol (190 mL) and H₂O (190 mL) was stirred at 30 °C for 1 h. The mixture was neutralized by the addition of 1.0 M hydrochloric acid. The resultant precipitate was collected by filtration and dried to give compounds **4a-4f**.

4-(2-Fluorophenylamino)-7-methoxyquinazolin-6-ol (4a)

Yellow powder, yield: 53%. ¹H-NMR (300 MHz; CDCl₃): 3.70 (s, 3H); 7.18 (s, 1H); 7.40-7.71 (m, 4H); 8.19 (s, 1H); 8.62 (s, 1H); 9.43 (s, 1H); 9.52 (s, 1H). MS (ESI⁺) *m/z* 286.0 (M+H)⁺.

4-(4-Fluorophenylamino)-7-methoxyquinazolin-6-ol (4b)

Yellow powder, yield: 60%. ¹H-NMR (300 MHz; CDCl₃): 3.71 (s, 3H); 7.19 (s, 1H); 7.41 (d, *J* = 8.4 Hz, 2H); 7.82 (d, *J* = 8.1 Hz, 2H); 8.21 (s, 1H); 8.58 (s, 1H); 9.46 (s, 1H). MS (ESI⁺) *m/z* 286.0 (M+H)⁺.

4-(2-Chlorophenylamino)-7-methoxyquinazolin-6-ol (4c)

Yellow powder, yield: 55%. ¹H-NMR (300 MHz; CDCl₃): 3.73 (s, 3H); 7.26 (s, 1H); 7.44-7.56 (m, 2H); 7.76-7.86 (m, 2H); 8.13 (s, 1H); 8.66 (s, 1H); 9.39 (s, 1H); 9.59 (s, 1H). MS (ESI⁺) *m/z* 302.0 (M+H)⁺.

4-(4-Chlorophenylamino)-7-methoxyquinazolin-6-ol (4d)

Yellow powder, yield: 53%. ¹H-NMR (300 MHz; CDCl₃): 3.71 (s, 3H); 7.26 (s, 1H); 7.43 (d, *J* = 8.4 Hz, 2H); 7.84 (d, *J* = 8.7 Hz, 2H); 8.12 (s, 1H); 8.61 (s, 1H); 9.45 (s, 1H). MS (ESI⁺) *m/z* 302.0 (M+H)⁺.

4-(2-Bromophenylamino)-7-methoxyquinazolin-6-ol (4e)

Yellow powder, yield: 52%. ¹H-NMR (300 MHz; CDCl₃): 3.69 (s, 3H); 7.12 (s,

1H); 7.37 (d, J = 8.4 Hz, 2H); 7.78 (d, J = 8.1 Hz, 1H); 7.82 (d, J = 8.4 Hz, 1H); 8.11 (s, 1H); 8.58 (s, 1H); 9.52 (s, 1H). MS (ESI⁺) m/z 346.0 (M+H)⁺.

4-(4-Bromophenylamino)-7-methoxyquinazolin-6-ol (4f)

Yellow powder, yield: 62%. ¹H-NMR (300 MHz; CDCl₃): 3.71 (s, 3H); 7.26 (s, 1H); 7.42 (d, J = 8.1 Hz, 2H); 7.83 (d, J = 8.1 Hz, 2H); 8.13 (s, 1H); 8.71 (s, 1H); 9.42 (s, 1H); 9.69 (s, 1H). MS (ESI⁺) m/z 302.0 (M+H)⁺.

4.1.4. General procedure for the preparation of the ethyl esters 5aa-4fd

A mixture of 7-methoxy-4-(phenylamino)quinazolin-6-ol derivatives **4a-4f** (0.87 mmol), appropriate ethyl bromoalkanoate (3.48 mmol), and potassium carbonate (0.3g, 2.18 mmol) in DMF (20 mL) was stirred at 40 °C for 4 h. The reaction mixture was filtered, and the filtrate was poured into ice water (200 mL) and extracted with ethyl acetate (3×50 mL). The combined organic extract was washed with brine, dried over Na₂SO₄, and filtered and the filtrate was evaporated in vacuo. The residue was washed with diethyl ether and dried to give compounds **5aa-5fd**.

Ethyl 4-(4-(2-fluorophenylamino)-7-methoxyquinazolin-6-yloxy)butanoate (5aa)

Yellow powder, yield: 67%. ¹H-NMR (300 MHz; *d*₆-DMSO): 1.28 (t, J = 6.9 Hz, 3H); 1.57-1.62 (m, 2H); 2.30 (t, J = 6.9 Hz, 2H); 3.88 (s, 3H); 4.15-4.20 (m, 4H); 7.19 (s, 1H); 7.42-7.84 (m, 5H); 8.13 (s, 1H); 8.45 (s, 1H). MS (ESI⁺) m/z 400.1 (M+H)⁺.

Ethyl 5-(4-(2-fluorophenylamino)-7-methoxyquinazolin-6-yloxy)pentanoate (5ab)

Pale yellow powder, yield: 66%. ¹H-NMR (300 MHz; *d*₆-DMSO): 1.31 (t, J = 6.3 Hz, 3H); 1.91-2.02 (m, 4H); 2.44 (t, J = 6.3 Hz, 2H); 3.93 (s, 3H); 4.13 (t, J = 6.6 Hz, 2H); 4.24 (t, J = 6.9 Hz, 2H); 7.48-7.59 (m, 4H); 7.84 (s, 1H); 8.12 (s, 1H); 8.26 (s, 1H); 8.48 (s, 1H). MS (ESI⁺) m/z 414.2 (M+H)⁺.

Ethyl 6-(4-(2-fluorophenylamino)-7-methoxyquinazolin-6-yloxy)hexanoate (5ac)

Yellow powder, yield: 70%. ¹H-NMR (300 MHz; *d*₆-DMSO): 1.31 (t, J = 6.6 Hz, 3H); 1.32-1.35 (m, 2H), 1.64-1.72 (m, 4H); 2.44 (t, J = 6.6 Hz, 2H); 3.93 (s, 3H); 4.13-4.24 (m, 4H); 7.48-7.59 (m, 4H); 7.84 (s, 1H); 8.12 (s, 1H); 8.26 (s, 1H); 8.46 (s, 1H). MS (ESI⁺) m/z 428.2 (M+H)⁺.

Ethyl 7-(4-(2-fluorophenylamino)-7-methoxyquinazolin-6-yloxy)heptanoate (5ad)

Yellow powder, yield: 74%. ¹H-NMR (300 MHz; *d*₆-DMSO): 1.38 (t, *J* = 6.3 Hz, 3H); 1.35-1.37 (m, 2H), 1.47-1.53 (m, 4H); 1.65-1.67 (m, 2H); 2.46 (t, *J* = 6.9 Hz, 2H); 3.97 (s, 3H); 4.15-4.18 (m, 4H); 7.23 (s, 1H); 7.45-7.84 (m, 5H); 8.18 (s, 1H); 8.56 (s, 1H). MS (ESI⁺) *m/z* 442.1 (M+H)⁺.

Ethyl 4-(4-(4-fluorophenylamino)-7-methoxyquinazolin-6-yloxy)butanoate (5ba)

Yellow powder, yield: 62%. ¹H-NMR (300 MHz; *d*₆-DMSO): 1.26 (t, *J* = 6.6 Hz, 3H); 1.70-1.78 (m, 2H); 2.45 (t, *J* = 6.6 Hz, 2H); 3.94 (s, 3H); 4.14 (t, *J* = 6.3 Hz, 2H); 4.23 (t, *J* = 6.9 Hz, 2H); 7.28 (d, *J* = 8.1 Hz, 2H); 7.35 (s, 1H); 7.45 (d, *J* = 8.7 Hz, 2H); 7.85 (s, 1H); 8.16 (s, 1H); 8.64 (s, 1H). MS (ESI⁺) *m/z* 400.1 (M+H)⁺.

Ethyl 5-(4-(4-fluorophenylamino)-7-methoxyquinazolin-6-yloxy)pentanoate (5bb)

Pale yellow powder, yield: 65%. ¹H-NMR (300 MHz; *d*₆-DMSO): 1.23 (t, *J* = 6.6 Hz, 3H); 1.97-2.02 (m, 4H); 2.45 (t, *J* = 6.3 Hz, 2H); 3.94 (s, 3H); 4.13-4.22 (m, 4H); 7.23 (s, 1H); 7.43 (d, *J* = 8.4 Hz, 2H); 7.84 (d, *J* = 8.4 Hz, 2H); 8.14 (s, 1H); 8.26 (s, 1H); 8.63 (s, 1H). MS (ESI⁺) *m/z* 414.1 (M+H)⁺.

Ethyl 6-(4-(4-fluorophenylamino)-7-methoxyquinazolin-6-yloxy)hexanoate (5bc)

Yellow powder, yield: 70%. ¹H-NMR (300 MHz; *d*₆-DMSO): 1.24 (t, *J* = 6.3 Hz, 3H); 1.60-1.68 (m, 4H); 1.83-1.86 (m, 2H); 2.44 (t, *J* = 6.6 Hz, 2H); 3.93 (s, 3H); 4.14-4.17 (m, 4H); 7.24 (s, 1H); 7.48 (d, *J* = 8.1 Hz, 2H); 7.92 (d, *J* = 8.1 Hz, 2H); 8.15 (s, 1H); 8.23 (s, 1H); 8.64 (s, 1H). MS (ESI⁺) *m/z* 428.1 (M+H)⁺.

Ethyl 7-(4-(4-fluorophenylamino)-7-methoxyquinazolin-6-yloxy)heptanoate (5bd)

Yellow powder, yield: 73%. ¹H-NMR (300 MHz; *d*₆-DMSO): 1.24 (t, *J* = 6.6 Hz, 3H); 1.34-1.38 (m, 2H); 1.53-1.57 (m, 2H); 1.63-1.73 (m, 4H); 2.43 (t, *J* = 6.6 Hz, 2H); 3.95 (s, 3H); 4.14-4.23 (m, 4H); 7.25 (s, 1H); 7.45 (d, *J* = 8.1 Hz, 2H); 7.86 (d, *J* = 8.4 Hz, 2H); 7.95 (s, 1H); 8.16 (s, 1H); 8.53 (s, 1H). MS (ESI⁺) *m/z* 442.1 (M+H)⁺.

Ethyl 4-(4-(2-chlorophenylamino)-7-methoxyquinazolin-6-yloxy)butanoate (5ca)

Yellow powder, yield: 66%. ¹H-NMR (300 MHz; *d*₆-DMSO): 1.31 (t, *J* = 6.9 Hz, 3H); 1.57-1.61 (m, 2H); 2.43 (t, *J* = 6.3 Hz, 2H); 3.92 (s, 3H); 4.15-4.22 (m, 4H); 7.24 (s, 1H); 7.43-7.56 (m, 4H); 7.83 (d, *J* = 8.7 Hz, 1H); 8.14 (s, 1H); 8.64 (s, 1H). MS

(ESI⁺) *m/z* 416.1 (M+H)⁺.

Ethyl 5-(4-(2-chlorophenylamino)-7-methoxyquinazolin-6-yloxy)pentanoate (5cb)

Yellow powder, yield: 65%. ¹H-NMR (300 MHz; *d*₆-DMSO): 1.31 (t, *J* = 6.3 Hz, 3H); 2.12-2.18 (m, 4H); 2.46 (t, *J* = 6.6 Hz, 2H); 3.93 (s, 3H); 4.14-4.23 (m, 4H); 7.24 (s, 1H); 7.73-7.85 (m, 2H); 7.89-7.96 (m, 3H); 8.14 (s, 1H); 8.32 (s, 1H); 8.63 (s, 1H). MS (ESI⁺) *m/z* 430.1 (M+H)⁺.

Ethyl 6-(4-(2-chlorophenylamino)-7-methoxyquinazolin-6-yloxy)hexanoate (5cc)

Pale yellow powder, yield: 72%. ¹H-NMR (300 MHz; *d*₆-DMSO): 1.31 (t, *J* = 6.3 Hz, 3H); 1.46-1.56 (m, 2H); 1.64-1.68 (m, 4H); 2.43 (t, *J* = 6.3 Hz, 2H); 3.94 (s, 3H); 4.13-4.22 (m, 4H); 7.23 (s, 1H); 7.42-7.45 (m, 2H); 7.42-7.47 (m, 2H); 7.87 (s, 1H); 8.13 (s, 1H); 8.52 (s, 1H). MS (ESI⁺) *m/z* 444.1 (M+H)⁺.

Ethyl 7-(4-(2-chlorophenylamino)-7-methoxyquinazolin-6-yloxy)heptanoate (5cd)

Pale yellow powder, yield: 45%. ¹H-NMR (300 MHz; *d*₆-DMSO): 1.32 (t, *J* = 6.3 Hz, 3H); 1.44-1.62 (m, 6H); 1.71-1.75 (m, 2H); 2.47 (t, *J* = 6.3 Hz, 2H); 3.94 (s, 3H); 4.14-4.24 (m, 4H); 7.23 (s, 1H); 7.45-7.63 (m, 4H); 7.86 (s, 1H); 8.22 (s, 1H); 8.73 (s, 1H). MS (ESI⁺) *m/z* 458.1 (M+H)⁺.

Ethyl 4-(4-(4-chlorophenylamino)-7-methoxyquinazolin-6-yloxy)butanoate (5da)

Yellow powder, yield: 52%. ¹H-NMR (300 MHz; *d*₆-DMSO): 1.28 (t, *J* = 6.6 Hz, 3H); 1.54-1.58 (m, 2H); 2.41 (t, *J* = 6.6 Hz, 2H); 3.93 (s, 3H); 4.13 (t, *J* = 6.3 Hz, 2H); 4.23 (d, *J* = 6.0 Hz, 2H); 7.24 (s, 1H); 7.44 (d, *J* = 8.1 Hz, 2H); 7.85 (d, *J* = 8.4 Hz, 2H); 8.14 (s, 1H); 8.23 (s, 1H); 8.56 (s, 1H). MS (ESI⁺) *m/z* 416.1 (M+H)⁺.

Ethyl 5-(4-(4-chlorophenylamino)-7-methoxyquinazolin-6-yloxy)pentanoate (5db)

Pale yellow powder, yield: 72%. ¹H-NMR (300 MHz; *d*₆-DMSO): 1.26 (t, *J* = 6.3 Hz, 3H); 1.86-1.97 (m, 4H); 2.34 (t, *J* = 6.9 Hz, 2H); 3.92 (s, 3H); 4.13 (t, *J* = 6.3 Hz, 2H); 4.23 (d, *J* = 6.6 Hz, 2H); 7.23 (s, 1H); 7.46 (d, *J* = 8.4 Hz, 2H); 7.82 (d, *J* = 8.1 Hz, 2H); 8.12 (s, 1H); 8.16 (s, 1H); 8.679 (s, 1H). MS (ESI⁺) *m/z* 430.2 (M+H)⁺.

Ethyl 6-(4-(4-chlorophenylamino)-7-methoxyquinazolin-6-yloxy)hexanoate (5dc)

Pale yellow powder, yield: 70%. ¹H-NMR (300 MHz; *d*₆-DMSO): 1.19 (t, *J* = 6.3 Hz, 3H); 1.64-1.71(m, 6H); 2.41 (t, *J* = 6.6 Hz, 2H); 3.94 (s, 3H); 4.15-4.23 (m, 4H); 7.24 (s, 1H); 7.48 (d, *J* = 8.4 Hz, 2H); 7.83 (s, 1H); 8.02 (s, 1H); 8.14 (d, *J* = 8.4 Hz, 2H); 8.64 (s, 1H). MS (ESI⁺) *m/z* 444.1 (M+H)⁺.

Ethyl 7-(4-(4-chlorophenylamino)-7-methoxyquinazolin-6-yloxy)heptanoate (5dd)

Yellow powder, yield: 53%. ¹H-NMR (300 MHz; *d*₆-DMSO): 1.38 (t, *J* = 6.3 Hz, 3H); 1.45-1.49 (m, 2H); 1.57-1.61 (m, 2H); 1.64-1.81 (m, 4H); 2.44 (t, *J* = 6.6 Hz, 2H); 3.92 (s, 3H); 4.12-4.17 (m, 4H); 7.24 (s, 1H); 7.46 (d, *J* = 8.7 Hz, 2H); 7.85 (d, *J* = 8.7 Hz, 2H); 8.15 (s, 1H); 8.58 (s, 1H); 8.62(s, 1H). MS (ESI⁺) *m/z* 458.1 (M+H)⁺.

Ethyl 4-(4-(2-bromophenylamino)-7-methoxyquinazolin-6-yloxy)butanoate (5ea)

Yellow powder, yield: 61%. ¹H-NMR (300 MHz; *d*₆-DMSO): 1.31 (t, *J* = 6.9 Hz, 3H); 1.76-1.80 (m, 2H); 2.45 (t, *J* = 6.9 Hz, 2H); 3.94 (s, 3H); 4.12 (t, *J* = 6.6 Hz, 2H); 4.23 (d, *J* = 6.0 Hz, 2H); 7.24 (s, 1H); 7.45-7.52(m, 3H); 7.85 (t, *J* = 8.4 Hz, 1H); 7.96 (s, 1H); 8.15 (d, *J* = 8.4 Hz, 1H); 8.53 (s, 1H). MS (ESI⁺) *m/z* 460.1 (M+H)⁺.

Ethyl 5-(4-(2-bromophenylamino)-7-methoxyquinazolin-6-yloxy)pentanoate (5eb)

Yellow powder, yield: 63%. ¹H-NMR (300 MHz; *d*₆-DMSO): 1.31 (t, *J* = 6.6 Hz, 3H); 1.87-1.92 (m, 4H); 2.45 (t, *J* = 6.9 Hz, 2H); 3.92 (s, 3H); 4.12-4.23 (m, 4H); 7.25 (s, 1H); 7.43-7.68 (m, 3H); 7.74 (s, 1H); 8.22 (s, 1H); 8.35 (s, 1H); 8.56 (s, 1H). MS (ESI⁺) *m/z* 474.1 (M+H)⁺.

Ethyl 6-(4-(2-bromophenylamino)-7-methoxyquinazolin-6-yloxy)hexanoate (5ec)

Pale yellow powder, yield: 45%. ¹H-NMR (300 MHz; *d*₆-DMSO): 1.31 (t, *J* = 6.9 Hz, 3H); 1.57-1.66 (m, 4H); 1.71-1.73 (m, 2H); 2.33 (t, *J* = 6.6 Hz, 2H); 3.92 (s, 3H); 4.13-4.22 (m, 4H); 7.23 (s, 1H); 7.48-7.82 (m, 4H); 7.99 (s, 1H); 8.16 (s, 1H); 8.63 (s, 1H). MS (ESI⁺) *m/z* 488.1 (M+H)⁺.

Ethyl 7-(4-(2-bromophenylamino)-7-methoxyquinazolin-6-yloxy)heptanoate (5ed)

Pale yellow powder, yield: 70%. ¹H-NMR (300 MHz; *d*₆-DMSO): 1.37 (t, *J* = 6.6 Hz, 3H); 1.45-1.47 (m, 2H); 1.56-1.74 (m, 6H); 2.46 (t, *J* = 6.3 Hz, 2H); 3.98 (s,

3H); 4.16-4.22 (m, 4H); 7.261 (s, 1H); 7.46 (d, $J = 8.4$ Hz, 2H); 7.58-7.63 (m, 2H); 7.95 (s, 1H); 8.19 (s, 1H); 8.641 (s, 1H). MS (ESI⁺) m/z 488.1 (M+H)⁺.

Ethyl 4-(4-(4-bromophenylamino)-7-methoxyquinazolin-6-yloxy)butanoate (5fa)

Pale yellow powder, yield: 63%. ¹H-NMR (300 MHz; *d*₆-DMSO): 1.30 (t, $J = 6.9$ Hz, 3H); 1.56-1.60 (m, 2H); 2.43 (d, $J = 6.6$ Hz, 2H); 3.91 (s, 3H); 4.12 (t, $J = 6.6$ Hz, 2H); 4.18-4.22 (m, 2H); 7.23 (s, 1H); 7.43 (d, $J = 8.7$ Hz, 2H); 7.84 (d, $J = 8.7$ Hz, 2H); 8.15 (s, 1H); 8.52 (s, 1H). MS (ESI⁺) m/z 460.2 (M+H)⁺.

Ethyl 5-(4-(4-bromophenylamino)-7-methoxyquinazolin-6-yloxy)pentanoate (5fb)

Yellow powder, yield: 66%. ¹H-NMR (300 MHz; *d*₆-DMSO): 1.33 (t, $J = 6.6$ Hz, 3H); 1.71-1.76 (m, 4H); 2.42 (t, $J = 6.3$ Hz, 2H); 3.94 (s, 3H); 4.13-4.18 (m, 4H); 7.24 (s, 1H); 7.45 (d, $J = 8.4$ Hz, 2H); 7.87 (d, $J = 8.4$ Hz, 2H); 8.13 (s, 1H); 8.66 (s, 1H). MS (ESI⁺) m/z 474.1 (M+H)⁺.

Ethyl 6-(4-(4-bromophenylamino)-7-methoxyquinazolin-6-yloxy)hexanoate (5fc)

Pale yellow powder, yield: 68%. ¹H-NMR (300 MHz; *d*₆-DMSO): 1.30 (t, $J = 6.6$ Hz, 3H); 1.56-1.63 (m, 4H); 1.82-1.84 (m, 2H); 2.44 (t, $J = 6.9$ Hz, 2H); 3.92 (s, 3H); 4.15-4.23 (m, 4H); 7.24 (s, 1H); 7.45 (d, $J = 8.7$ Hz, 2H); 7.84 (d, $J = 8.7$ Hz, 2H); 7.91 (s, 1H); 8.16 (s, 1H); 8.55 (s, 1H). MS (ESI⁺) m/z 488.1 (M+H)⁺.

Ethyl 7-(4-(4-bromophenylamino)-7-methoxyquinazolin-6-yloxy)heptanoate (5fd)

Pale yellow powder, yield: 72%. ¹H-NMR (300 MHz; *d*₆-DMSO): 1.28 (t, $J = 6.6$ Hz, 3H); 1.34-1.37 (m, 2H); 1.53-1.67 (m, 6H); 2.54 (t, $J = 6.7$ Hz, 2H); 3.95 (s, 3H); 4.12 (t, $J = 6.3$ Hz, 2H); 4.28 (d, $J = 6.6$ Hz, 2H); 7.33 (s, 1H); 7.60 (d, $J = 8.4$ Hz, 2H); 7.78 (d, $J = 8.7$ Hz, 2H); 7.90 (s, 1H); 8.15 (s, 1H); 8.62 (s, 1H). MS (ESI⁺) m/z 502.1 (M+H)⁺.

4.1.5. General procedure for the preparation of the title compounds 6aa-6fd

A solution of potassium hydroxide (5.6 g, 100 mmol) in methanol (14 mL) was added to a stirred solution of hydroxylamine hydrochloride (4.67 g, 67.2 mmol) in methanol (24 mL) at 0 °C. The reaction mixture was stirred at 0 °C for 1 h. The

precipitate was removed by filtration and the filtrate was collected to provide fresh hydroxylamine solution which was stored in a refrigerator before use. The appropriate esters **5aa-5fd** (10 mmol) was added to the above freshly prepared hydroxylamine solution (30 mL) at 0 °C. The reaction mixture was stirred at room temperature for 24 h. The reaction mixture was neutralized with acetic acid. The formed precipitate was collected by filtration, washed with water, and dried in vacuo to give the title compounds.

4-(4-(2-fluorophenylamino)-7-methoxyquinazolin-6-yloxy)-N-hydroxybutanamide (6aa)

Pale yellow powder, yield: 36%, mp: 195-197 °C. ¹H-NMR (300 MHz; *d*₆-DMSO): 2.06 (t, *J* = 6.9 Hz, 2H); 2.21 (t, *J* = 6.9 Hz, 2H); 3.94 (s, 3H); 4.15 (t, *J* = 5.1 Hz); 7.20 (s, 1H); 7.43 (d, *J* = 8.4 Hz, 2H); 7.88 (t, *J* = 8.4 Hz, 2H); 8.48 (s, 1H); 8.72 (s, 1H); 9.52 (s, 1H); 10.47 (s, 1H). MS (ESI⁺) *m/z* 387.2 (M+H)⁺. Anal. Calcd for C₁₉H₁₉FN₄O₄: C, 59.06; H, 4.96; N, 14.50; Found: C, 59.34; H, 4.92; N, 14.58.

5-(4-(2-fluorophenylamino)-7-methoxyquinazolin-6-yloxy)-N-hydroxypentanamide (6ab)

Pale yellow powder, yield: 32%, mp: 235-237 °C. ¹H-NMR (300 MHz; *d*₆-DMSO): 1.70-1.83 (m, 4H); 2.07 (t, *J* = 6.4 Hz, 2H); 4.02 (s, 3H); 4.21 (t, *J* = 6.3 Hz, 2H); 7.32-7.59 (m, 5H); 8.25 (s, 1H); 8.79 (s, 1H); 10.429 (s, 1H). MS (ESI⁺) *m/z* 401.2 (M+H)⁺. Anal. Calcd for C₂₀H₂₁FN₄O₄: C, 59.99; H, 5.29; N, 13.99; Found: C, 59.78; H, 5.33; N, 14.02.

6-(4-(2-fluorophenylamino)-7-methoxyquinazolin-6-yloxy)-N-hydroxyhexanamide (6ac)

Pale yellow powder, yield: 40%, mp: 220-223 °C. ¹H-NMR (300 MHz; *d*₆-DMSO): 1.25-1.30 (m, 2H); 1.44-1.46 (m, 2H); 1.58-1.62 (m, 2H); 2.00 (t, *J* = 6.9 Hz, 2H); 4.01 (s, 3H); 4.20 (t, *J* = 6.2 Hz, 2H); 7.32-7.59 (m, 5H); 8.25 (s, 1H); 8.79 (s, 1H); 10.40 (s, 1H). MS (ESI⁺) *m/z* 415.2 (M+H)⁺. Anal. Calcd for C₂₁H₂₃FN₄O₄: C, 60.86; H, 5.59; N, 13.52; Found: C, 61.13; H, 5.64; N, 13.60.

7-(4-(2-fluorophenylamino)-7-methoxyquinazolin-6-yloxy)-N-hydroxyheptanamide (6ad)

Pale yellow powder, yield: 35%, mp: 165-167 °C. ¹H-NMR (300 MHz; *d*₆-DMSO): 1.26-1.56 (m, 6H); 1.83 (s, 2H); 1.97 (t, *J* = 6.6 Hz, 2H); 4.01 (s, 3H); 4.18 (t, *J* = 6.4 Hz, 2H); 7.35-7.58 (m, 5H); 8.22 (s, 1H); 8.78 (s, 1H); 10.36 (s, 1H). MS (ESI⁺) *m/z* 429.2 (M+H)⁺. Anal. Calcd for C₂₂H₂₅FN₄O₄: C, 61.67; H, 5.88; N, 13.08; Found: C, 61.55; H, 5.85; N, 13.14.

4-(4-(4-fluorophenylamino)-7-methoxyquinazolin-6-yloxy)-N-hydroxybutanamide (6ba)

Yellow powder, yield: 52%, mp: 216-218 °C. ¹H-NMR (300 MHz; *d*₆-DMSO): 2.06 (t, *J* = 6.3 Hz, 2H); 2.22 (t, *J* = 6.0 Hz, 2H); 3.94 (s, 3H); 4.07-4.15 (m, 2H); 7.19-7.25 (m, 3H); 7.76-7.86 (m, 2H); 8.41 (s, 1H); 8.72 (s, 1H); 9.50 (s, 1H); 10.47 (s, 1H). MS (ESI⁺) *m/z* 387.2 (M+H)⁺. Anal. Calcd for C₁₉H₁₉FN₄O₄: C, 59.06; H, 4.96; N, 14.50; Found: C, 58.73; H, 4.93; N, 14.46.

5-(4-(4-fluorophenylamino)-7-methoxyquinazolin-6-yloxy)-N-hydroxypentanamide (6bb)

Pale yellow powder, yield: 54%, mp: 236-238 °C. ¹H-NMR (300 MHz; *d*₆-DMSO): 1.70-1.82 (m, 4H); 2.05 (t, *J* = 6.3 Hz, 2H); 3.94 (s, 3H); 4.15 (t, *J* = 6.0 Hz, 2H); 7.19-7.26 (m, 3H); 7.75-7.85 (m, 2H); 8.45 (s, 1H); 8.70 (s, 1H); 9.71 (s, 1H); 10.39 (s, 1H). MS (ESI⁺) *m/z* 401.2 (M+H)⁺. Anal. Calcd for C₂₀H₂₁FN₄O₄: C, 59.99; H, 5.29; N, 13.99; Found: C, 60.25; H, 5.32; N, 14.04.

6-(4-(4-fluorophenylamino)-7-methoxyquinazolin-6-yloxy)-N-hydroxyhexanamide (6bc)

Pale yellow powder, yield: 52%, mp: 198-200 °C. ¹H-NMR (300 MHz; *d*₆-DMSO): 1.45 (s, 2H); 1.60 (t, *J* = 6.9 Hz, 2H); 1.82 (d, *J* = 6.6 Hz, 2H); 2.00 (t, *J* = 6.9 Hz, 2H); 3.97 (s, 3H); 4.16 (t, *J* = 6.3 Hz, 2H); 7.24 (s, 1H); 7.49 (d, *J* = 8.7 Hz, 2H); 7.81 (d, *J* = 8.7 Hz, 2H); 7.98 (s, 1H); 8.63 (s, 1H); 10.39 (s, 1H). MS (ESI⁺) *m/z* 415.2 (M+H)⁺. Anal. Calcd for C₂₁H₂₃FN₄O₄: C, 60.86; H, 5.59; N, 13.52; Found: C, 61.16; H, 5.56; N, 13.45.

7-(4-(4-fluorophenylamino)-7-methoxyquinazolin-6-yloxy)-N-hydroxyheptanamide (6bd)

Yellow powder, yield: 43%, mp: 251-253 °C. ¹H-NMR (300 MHz; *d*₆-DMSO):

1.34-1.56 (m, 6H); 1.81 (d, $J = 6.9$ Hz, 2H); 1.97 (t, $J = 6.9$ Hz, 2H); 4.00 (s, 3H); 4.20 (t, $J = 6.3$ Hz, 2H); 7.30-7.36 (m, 3H); 7.68-7.73 (m, 2H); 8.23 (s, 1H); 8.79 (s, 1H); 10.36 (s, 1H). MS (ESI⁺) m/z 429.3 (M+H)⁺. Anal. Calcd for C₂₂H₂₅FN₄O₄: C, 61.67; H, 5.88; N, 13.08; Found: C, 61.89; H, 5.91; N, 13.14.

4-(4-(2-chlorophenylamino)-7-methoxyquinazolin-6-yloxy)-N-hydroxybutanamide (6ca)

Pale yellow powder, yield: 57%, mp: 210-212 °C. ¹H-NMR (300 MHz; *d*₆-DMSO): 2.08 (t, $J = 6.6$ Hz, 2H); 2.22 (d, $J = 6.6$ Hz, 2H); 4.00 (s, 3H); 4.22 (t, $J = 6.2$ Hz, 2H); 7.32 (s, 1H); 7.64-7.79 (m, 4H); 8.19 (s, 1H); 8.78 (s, 1H); 10.48 (s, 1H). MS (ESI⁺) m/z 403.1 (M+H)⁺. Anal. Calcd for C₁₉H₁₉ClN₄O₄: C, 56.65; H, 4.75; N, 13.91; Found: C, 56.79; H, 4.71; N, 13.86.

5-(4-(2-chlorophenylamino)-7-methoxyquinazolin-6-yloxy)-N-hydroxypentanamide (6cb)

Pale yellow powder, yield: 52%, mp: 168-170 °C. ¹H-NMR (300 MHz; *d*₆-DMSO): 1.71-1.83 (m, 4H); 2.09 (s, 2H); 3.98 (s, 3H); 4.17 (s, 2H); 7.25 (s, 1H); 7.40-7.49 (m, 2H); 7.55-7.64 (m, 2H); 7.99 (s, 1H); 8.53 (s, 1H); 10.36 (s, 1H). MS (ESI⁺) m/z 417.2 (M+H)⁺. Anal. Calcd for C₂₀H₂₁ClN₄O₄: C, 57.62; H, 5.08; N, 13.44; Found: C, 57.85; H, 5.12; N, 13.49.

6-(4-(2-chlorophenylamino)-7-methoxyquinazolin-6-yloxy)-N-hydroxyhexanamide (6cc)

Pale yellow powder, yield: 48%, mp: 193-194 °C. ¹H-NMR (300 MHz; *d*₆-DMSO): 1.45 (d, $J = 5.2$ Hz, 2H); 1.60-2.09 (m, 6H); 3.96 (s, 3H); 4.12 (s, 2H); 7.21 (s, 1H); 7.36-7.47 (m, 2H); 7.54-7.62 (m, 2H); 8.42 (s, 1H); 8.68 (s, 1H); 9.98 (s, 1H); 10.36 (s, 1H). MS (ESI⁺) m/z 431.1 (M+H)⁺. Anal. Calcd for C₂₁H₂₃ClN₄O₄: C, 58.54; H, 5.38; N, 13.00; Found: C, 58.32; H, 5.42; N, 12.96.

7-(4-(2-chlorophenylamino)-7-methoxyquinazolin-6-yloxy)-N-hydroxyheptanamide (6cd)

Pale yellow powder, yield: 36%, mp: 185-187 °C. ¹H-NMR (300 MHz; *d*₆-DMSO): 1.34-1.56 (m, 6H); 1.82 (d, $J = 6.6$ Hz, 2H); 1.97 (t, $J = 6.9$ Hz, 2H); 4.00 (s, 3H); 4.17 (t, $J = 6.3$ Hz, 2H); 7.29 (s, 1H); 7.44-7.68 (m, 4H); 8.09 (s, 1H); 8.67 (s,

1H); 10.35 (s, 1H). MS (ESI⁺) *m/z* 445.1 (M+H)⁺. Anal. Calcd for C₂₂H₂₅ClN₄O₄: C, 59.39; H, 5.66; N, 12.59; Found: C, 59.64; H, 5.61; N, 12.53.

4-(4-(4-chlorophenylamino)-7-methoxyquinazolin-6-yloxy)-N-hydroxybutanamide (6da)

Yellow powder, yield: 64%, mp: 245-247 °C. ¹H-NMR (300 MHz; *d*₆-DMSO): 2.06 (t, *J* = 6.9 Hz, 2H); 2.22 (t, *J* = 7.2 Hz, 2H); 3.94 (s, 3H); 4.15 (t, *J* = 5.4 Hz, 2H); 7.20 (s, 1H); 7.43 (d, *J* = 8.4 Hz, 2H); 7.85-7.91 (m, 2H); 8.48 (s, 1H); 8.72 (s, 1H); 9.52 (s, 1H); 10.47 (s, 1H). MS (ESI⁺) *m/z* 403.2 (M+H)⁺. Anal. Calcd for C₁₉H₁₉ClN₄O₄: C, 56.65; H, 4.75; N, 13.91; Found: C, 56.82; H, 4.80; N, 13.98.

5-(4-(4-chlorophenylamino)-7-methoxyquinazolin-6-yloxy)-N-hydroxypentanamide (6db)

Pale yellow powder, yield: 63%, mp: 235-237 °C. ¹H-NMR (300 MHz; *d*₆-DMSO): 1.70-1.83 (m, 4H); 2.07 (t, *J* = 7.2 Hz, 2H); 3.99 (s, 3H); 4.20 (t, *J* = 6.0 Hz, 2H); 7.26 (s, 1H); 7.52 (d, *J* = 8.7 Hz, 2H); 7.78 (d, *J* = 8.7 Hz, 2H); 8.07 (s, 1H); 8.72 (s, 1H); 10.40 (s, 1H). MS (ESI⁺) *m/z* 417.2 (M+H)⁺. Anal. Calcd for C₂₀H₂₁ClN₄O₄: C, 57.62; H, 5.08; N, 13.44; Found: C, 57.36; H, 5.03; N, 13.51.

6-(4-(4-chlorophenylamino)-7-methoxyquinazolin-6-yloxy)-N-hydroxyhexanamide (6dc)

Pale yellow powder, yield: 45%, mp: 218-220 °C. ¹H-NMR (300 MHz; *d*₆-DMSO): 1.46 (d, *J* = 6.6 Hz, 2H); 1.60 (t, *J* = 6.9 Hz, 2H); 1.82 (t, *J* = 6.6 Hz, 2H); 2.00 (t, *J* = 6.9 Hz, 2H); 3.97 (s, 3H); 4.16 (t, *J* = 6.3 Hz, 2H); 7.24 (s, 1H), 7.49 (d, *J* = 8.7 Hz, 2H); 7.81 (d, *J* = 8.7 Hz, 2H); 7.98 (s, 1H); 8.63 (s, 1H); 10.37 (s, 1H). MS (ESI⁺) *m/z* 431.2 (M+H)⁺. Anal. Calcd for C₂₁H₂₃ClN₄O₄: C, 58.54; H, 5.38; N, 13.00; Found: C, 58.91; H, 5.43; N, 13.06.

7-(4-(4-chlorophenylamino)-7-methoxyquinazolin-6-yloxy)-N-hydroxyheptanamide (6dd)

Pale yellow powder, yield: 51%, mp: 238-240 °C. ¹H-NMR (300 MHz; *d*₆-DMSO): 1.34-1.53 (m, 6H); 1.83 (s, 2H); 1.96 (t, *J* = 7.2 Hz, 2H); 4.00 (s, 3H); 4.17 (t, *J* = 5.4 Hz, 2H); 7.28 (s, 1H); 7.55 (d, *J* = 8.4 Hz, 2H); 7.74 (d, *J* = 8.7 Hz, 2H); 8.12 (s, 1H); 8.79 (s, 1H); 10.34 (s, 1H). MS (ESI⁺) *m/z* 445.2 (M+H)⁺. Anal.

Calcd for C₂₂H₂₅ClN₄O₄: C, 59.39; H, 5.66; N, 12.59; Found: C, 59.14; H, 5.63; N, 12.64.

4-(4-(2-bromophenylamino)-7-methoxyquinazolin-6-yloxy)-N-hydroxybutanamide (6ea)

Yellow powder, yield: 63%, mp: 183-186 °C. ¹H-NMR (300 MHz; *d*₆-DMSO): 2.06 (d, *J* = 7.2 Hz, 2H); 2.21 (d, *J* = 6.6 Hz, 2H); 3.97 (s, 3H); 4.14 (s, 2H); 7.22-7.54 (m, 4H); 7.70-7.79 (m, 1H); 7.94-7.99 (m, 1H); 8.46 (s, 1H); 10.45 (s, 1H). MS (ESI⁺) *m/z* 447.1 (M+H)⁺. Anal. Calcd for C₁₉H₁₉BrN₄O₄: C, 51.02; H, 4.28; N, 12.53; Found: C, 50.75; H, 4.30; N, 12.58.

5-(4-(2-bromophenylamino)-7-methoxyquinazolin-6-yloxy)-N-hydroxypentanamide (6eb)

Yellow powder, yield: 46%, mp: 195-197 °C. ¹H-NMR (300 MHz; *d*₆-DMSO): 1.73-1.82 (m, 4H); 2.09 (s, 2H); 3.94 (s, 3H); 4.13 (s, 2H); 7.19 (s, 1H); 7.28 (d, *J* = 7.2 Hz, 1H); 7.47-7.52 (m, 1H); 7.75 (d, *J* = 7.8 Hz, 1H); 7.85 (s, 1H); 8.33 (s, 1H); 8.69 (s, 1H); 9.63 (s, 1H); 10.38 (s, 1H). MS (ESI⁺) *m/z* 461.1 (M+H)⁺. Anal. Calcd for C₂₀H₂₁BrN₄O₄: C, 52.07; H, 4.59; N, 12.15; Found: C, 51.82; H, 4.63; N, 12.10.

6-(4-(2-bromophenylamino)-7-methoxyquinazolin-6-yloxy)-N-hydroxyhexanamide (6ec)

Yellow powder, yield: 50%, mp: 170-172 °C. ¹H-NMR (300 MHz; *d*₆-DMSO): 1.46 (d, *J* = 6.6 Hz, 2H); 1.60 (t, *J* = 6.9 Hz, 2H); 1.82 (d, *J* = 6.6 Hz, 2H); 2.00 (t, *J* = 6.9 Hz, 2H); 3.97 (s, 3H); 4.16 (t, *J* = 6.3 Hz, 2H); 7.24 (s, 1H); 7.49 (d, *J* = 8.7 Hz, 2H); 7.81 (d, *J* = 8.7 Hz, 2H); 7.98 (s, 1H); 8.63 (s, 1H); 10.37 (s, 1H). MS (ESI⁺) *m/z* 475.1 (M+H)⁺. Anal. Calcd for C₂₁H₂₃BrN₄O₄: C, 53.06; H, 4.88; N, 11.79; Found: C, 53.32; H, 4.92; N, 11.84.

7-(4-(2-bromophenylamino)-7-methoxyquinazolin-6-yloxy)-N-hydroxyheptanamide (6ed)

Yellow powder, yield: 44%, mp: 188-190 °C. ¹H-NMR (300 MHz; *d*₆-DMSO): 1.23-1.55 (m, 6H); 1.81 (d, *J* = 6.9 Hz, 2H); 1.95 (d, *J* = 7.2 Hz, 2H); 4.00 (s, 3H); 4.16 (t, *J* = 6.0 Hz, 2H); 7.31-7.38 (m, 2H); 7.43 (s, 2H); 7.81 (d, *J* = 8.1 Hz, 1H); 8.05 (d, *J* = 8.1 Hz, 1H); 8.67 (s, 1H); 10.35 (s, 1H). MS (ESI⁺) *m/z* 489.1 (M+H)⁺.

Anal. Calcd for C₂₂H₂₅BrN₄O₄: C, 54.00; H, 5.15; N, 11.45; Found: C, 54.26; H, 5.19; N, 11.50.

4-(4-(4-bromophenylamino)-7-methoxyquinazolin-6-yloxy)-N-hydroxybutanamide (6fa)

Yellow powder, yield: 54%, mp: 225-227 °C. ¹H-NMR (300 MHz; *d*₆-DMSO): 2.06 (t, *J* = 6.3 Hz, 2H); 2.21 (t, *J* = 6.6 Hz, 2H); 4.00 (s, 3H); 4.22 (s, 2H); 7.32 (s, 1H); 7.64-7.75(m, 4H); 8.19 (s, 1H); 8.78 (s, 1H); 10.48(s, 1H). MS (ESI⁺) *m/z* 447.1 (M+H)⁺. Anal. Calcd for C₁₉H₁₉BrN₄O₄: C, 51.02; H, 4.28; N, 12.53; Found: C, 51.26; H, 4.31; N, 12.49.

5-(4-(4-bromophenylamino)-7-methoxyquinazolin-6-yloxy)-N-hydroxypentanamide (6fb)

Yellow powder, yield: 35%, mp: 212-213 °C. ¹H-NMR (300 MHz; *d*₆-DMSO): 1.71-1.82 (m, 4H); 2.08 (s, 2H); 3.94 (s, 3H); 4.14 (d, *J* = 6.0 Hz, 2H); 7.20 (s, 1H); 7.56 (d, *J* = 8.7 Hz, 2H); 7.82 (d, *J* = 7.2 Hz, 2H); 8.47 (s, 1H); 8.69 (s, 1H); 9.50 (s, 1H); 10.39 (s, 1H). Anal. Calcd for C₂₀H₂₁BrN₄O₄: C, 52.07; H, 4.59; N, 12.15; Found: C, 52.30; H, 4.57; N, 12.11.

6-(4-(4-bromophenylamino)-7-methoxyquinazolin-6-yloxy)-N-hydroxyhexanamide (6fc)

Yellow powder, yield: 61%, mp: 225-226 °C. ¹H-NMR (300 MHz; *d*₆-DMSO): 1.45 (s, 2H); 1.61 (s, 2H); 1.83 (s, 2H); 1.99 (d, *J* = 6.9 Hz, 2H); 3.94 (s, 3H); 4.13 (s, 2H); 7.20 (s, 1H); 7.56 (d, *J* = 8.7 Hz, 2H); 7.81 (d, *J* = 6.0 Hz, 2H); 8.47 (s, 1H); 8.68 (s, 1H); 9.51 (s, 1H); 10.38 (s, 1H). MS (ESI⁺) *m/z* 475.1 (M+H)⁺. Anal. Calcd for C₂₁H₂₃BrN₄O₄: C, 53.06; H, 4.88; N, 11.79; Found: C, 53.29; H, 4.85; N, 11.74.

7-(4-(4-bromophenylamino)-7-methoxyquinazolin-6-yloxy)-N-hydroxyheptanamide (6fd)

Yellow powder, yield: 45%, mp: 235-237 °C. ¹H-NMR (300 MHz; *d*₆-DMSO): 1.34 (d, *J* = 6.3 Hz, 2H); 1.46-1.54 (m, 4H); 1.83 (s, 2H); 1.95 (d, *J* = 6.9 Hz, 2H); 4.00 (s, 3H); 4.19 (s, 2H); 7.28 (s, 1H); 7.69 (s, 4H); 8.12 (s, 1H); 8.78 (s, 1H); 10.35 (s, 1H). MS (ESI⁺) *m/z* 489.1 (M+H)⁺. Anal. Calcd for C₂₂H₂₅BrN₄O₄: C, 54.00; H, 5.15; N, 11.45; Found: C, 54.24; H, 5.18; N, 11.41.

4.2. VEGFR-2 Inhibition Assay

VEGFR-2 kinase inhibitory activity was measured using HTScan VEGF Receptor 2 Kinase Assay Kit (Cell Signaling Technology, Inc.) by colorimetric ELISA assay according to the manufacturer's instructions, as described previously by us [48]. Briefly, 12.5 μ L of the 4 \times reaction cocktail containing 100 ng VEGFR-2 was incubated with 12.5 μ L of various concentrations of tested compounds for 5 min at room temperature. 25 μ L of 2 \times ATP/gastrin precursor (Tyr87) biotinylated peptide cocktail was then added to the pre-incubated reaction cocktail. After incubation at room temperature for 30 min, 50 μ L of stop buffer (50 mM EDTA, pH 8) were added to each well to stop the reaction. After that, 25 μ L of each reaction were transferred into a 96-well streptavidin-coated plate containing 75 μ L H₂O/well and were incubated at room temperature for 60 min. Next, the wells were washed three times with 200 μ L/well PBS/T (0.05% Tween 20), after which 100 μ L of primary antibody [phosphorylated tyrosine monoclonal antibody (pTyr-100), 1:1000 in PBS/T with 1% bovine serum albumin (BSA)] was added per well. Following incubation at room temperature for 60 min, the wells were washed three times with 200 μ L/well of PBS/T. Next, 100 μ L secondary antibody (HRP labeled anti-mouse IgG, 1:500 in PBS/T with 1% BSA) was added per well. Following incubation at room temperature for 30 min, the wells were washed five times with 200 μ L/well of PBS/T. Subsequently, 100 μ L of TMB substrate were added per well, and the plate was incubated at room temperature for 15 min. After that, 100 μ L/well of stop solution was added, and the wells were mixed and incubated at room temperature for 20 min. The plate was then read at 450 nm with an ELISA microplate reader.

4.3. HDAC Inhibition Assay

HDAC inhibitory activity was measured using the Fluor de Lys HDAC fluorometric activity assay kit (Enzo Life Sciences, Inc.) as described elsewhere [44] with some modifications. Briefly, HeLa cell nuclear extracts or HDAC isoforms were incubated with various concentrations of compounds for 15 min at room temperature, and HDAC reaction was initiated by addition of Fluor de Lys substrate. The resulting

mixture was incubated for 1 h at room temperature, followed by adding developer to stop the reaction. Fluorescence was measured by a microplate reader (Synergy Mx) with excitation at 355 nm and emission at 460 nm. The assay was repeated three times independently.

4.4. Cell proliferation Assay

The antiproliferative activities of the prepared *N*-phenylquinazolin-4-amine hybrids against MCF-7 cells were evaluated by MTT assay, as described previously by us [48]. Briefly, MCF-7 cells were grown to log phase in RPMI 1640 medium supplemented with 10% fetal bovine serum. After diluting to 2×10^4 cells mL^{-1} with the complete medium, 100 μL of the obtained cell suspension was added to each well of 96-well culture plates. The subsequent incubation was permitted at 37 °C, 5% CO_2 atmosphere for 24 h before the antiproliferative assessments. Tested compounds at pre-set concentrations were added to 6 wells. After 48 h exposure period, 40 μL of PBS containing 2.5 mg mL^{-1} of MTT was added to each well. 100 μL extraction solution (10% SDS-5% isobutyl alcohol-0.010M HCl) was added after 4 h. After an overnight incubation at 37 °C, the optical density was measured at a wavelength of 570 nm on an ELISA microplate reader. The inhibition rate of tumor cells for each compound with different concentrations was calculated following the formula: inhibition rate (%) = $(1 - \text{OD}_{\text{compound exposure}} / \text{OD}_{\text{control}}) \times 100$. The IC_{50} value was defined as the concentration at which 50% survival of cells was occurred.

4.5. Molecular docking

Molecular docking of compound **6fd** into the three dimensional X-ray structure of VEGFR-2 (PDB code: 2QU5) and HDLP (HDAC homologue, PDB code: 1C3S) was carried out using the Discovery Studio (version 3.1) as implemented through the graphical user interface DiscoveryStudio CDOCKER protocol.

The three-dimensional structure of the compound **6fd** was constructed using ChemBio 3D Ultra 11.0 software [Chemical Structure Drawing Standard; Cambridge Soft corporation, USA (2008)], then it was energetically minimized by using MMFF94 with 5000 iterations and minimum RMS gradient of 0.10. The crystal

structures of VEGFR-2 kinase and HDLP were retrieved from the RCSB Protein Data Bank (<http://www.rcsb.org/pdb/home/home.-do>). All bound waters and ligands were eliminated and the polar hydrogen was added. The whole 2QU5 or 1C3S was defined as a receptor and the site sphere was selected based on the binding site of 2QU5 or 1C3S. Compound **6fd** were placed during the molecular docking procedure. Types of interactions of the docked protein with ligand were analyzed after the end of molecular docking.

Acknowledgements

This work was supported by National Natural Science Foundation of China (Grant No. 21102182), Natural Science Foundation of Jiangsu Province (Grant No. BK2012760), Research Fund of young scholars for the Doctoral Program of Higher Education of China (Grant No. 20110096120008), College Students Innovation Project for the R&D of Novel Drugs (Grant No. J1030830) and Youth development projects of Army Medical Technology (Grant No. 15QNP021).

References

- [1] W. Risau, Mechanisms of angiogenesis, *Nature* 386 (1997) 671-674.
- [2] P. Carmeliet, Angiogenesis in health and disease, *Nat. Med.* 9 (2003) 653-660.
- [3] D.A. Walsh, L. Haywood, Angiogenesis: a therapeutic target in arthritis, *Curr. Opin. Invest. Drugs* 2 (2001) 1054-1063.
- [4] M. Detmar, The role of VEGF and thrombospondins in skin angiogenesis, *J. Dermatol. Sci.* 24 (Suppl. 1) (2000) S78-S84.
- [5] L.P. Aiello, R.L. Avery, P.G. Arrigg, B.A. Keyt, H.D. Jampel, S.T. Shah, L.R. Pasquale, H. Thieme, M.A. Iwamoto, J.E. Park, H.V. Nguyen, L.M. Aiello, N. Ferrara, G.L. King, Vascular endothelial growth factor in ocular fluid of patients with diabetic retinopathy and other retinal disorders, *N. Engl. J. Med.* 331 (1994) 1480-1487.
- [6] R.S. Kerbel, Tumor angiogenesis, *N. Engl. J. Med.* 358 (2008) 2039-2049.
- [7] L.A. Liotta, P.S. Steeg, W.G. Stetler-Stevenson, Cancer metastasis and angiogenesis: an imbalance of positive and negative regulation, *Cell* 64 (1991) 327-336.

- [8] S. Shinkaruk, M. Bayle, G. Lain, G. Deleris, Vascular endothelial cell growth factor (VEGF), an emerging target for cancer chemotherapy. *Curr. Med. Chem.* 3 (2003) 95-117.
- [9] T. Veikkola, M. Karkkainen, L. Claesson-Welsh, K. Alitalo, Regulation of angiogenesis via vascular endothelial growth factor receptors. *Cancer Res.* 60 (2000) 203-212.
- [10] N. Ferrara, H.P. Gerber, J. LeCouter, The biology of VEGF and its receptors, *Nat. Med.* 9 (2003) 669-676.
- [11] A.K. Olsson, A. Dimberg, J. Kreuger, L. Claesson-Welsh, VEGF receptor signalling - in control of vascular function, *Nat. Rev. Mol. Cell Biol.* 7 (2006) 359-371.
- [12] A. Sandler, R. Gray, M.C. Perry, J. Brahmer, J.H. Schiller, A. Dowlati, R. Lilenbaum, D.H. Johnson, Paclitaxel-carboplatin alone or with bevacizumab for non-small-cell lung cancer, *N. Engl. J. Med.* 355 (2006) 2542–2550.
- [13] H. Hurwitz, L. Fehrenbacher, W. Novotny, T. Cartwright, J. Hainsworth, W. Heim, J. Berlin, A. Baron, S. Griffing, E. Holmgren, N. Ferrara, G. Fyfe, B. Rogers, R. Ross, F. Kabbinavar, Bevacizumab plus irinotecan, fluorouracil, and leucovorin for metastatic colorectal cancer, *N. Engl. J. Med.* 350 (2004) 2335–2342.
- [14] G. Aprile, E. Rijavec, C. Fontanella, K. Rihawi, F. Grossi, Ramucirumab: preclinical research and clinical development, *Onco. Targets Ther.* 7 (2014) 1997–2006.
- [15] M. Atkins, C.A. Jones, P. Kirkpatrick, Sunitinib malate, *Nat. Rev. Drug Discov.* 5 (2006) 279–280.
- [16] S. Wilhelm, C. Carter, M. Lynch, T. Lowinger, J. Dumas, R.A. Smith, B. Schwartz, R. Simantov, S. Kelley, Discovery and development of sorafenib: a multikinase inhibitor for treating cancer, *Nat. Rev. Drug Discov.* 5 (2006) 835–844.
- [17] H. Commander, G. Whiteside, C. Perry, Vandetanib: first global approval, *Drugs* 71 (2011) 1355–1365.
- [18] L.M. Ellis, D.J. Hicklin, Pathways Mediating Resistance to Vascular Endothelial Growth Factor–Targeted Therapy, *Clin Cancer Res.* 14 (2008) 6371-6375.
- [19] R.K. Jain, D.G. Duda, C.G. Willett, D.V. Sahani, A.X. Zhu, J.S. Loeffler, T.T. Batchelor, A.G. Sorensen, Biomarkers of response and resistance to antiangiogenic therapy, *Nat. Rev. Clin. Oncol.* 6 (2009) 327-338.
- [20] T. Arao, K. Matsumoto, K. Furuta, K. Kudo, H. Kaneda, T. Nagai, K. Sakai, Y.

- Fujita, D. Tamura, K. Aomatsu, F. Koizumi, K. Nishio, Acquired drug resistance to vascular endothelial growth factor receptor 2 tyrosine kinase inhibitor in human vascular endothelial cells, *Anticancer Res.* 31(9) (2011) 2787-2796.
- [21] J.M. Clarke, H.I. Hurwitz, Understanding and targeting resistance to anti-angiogenic therapies, *J. Gastrointest. Oncol.* 4(3) (2013) 253-263.
- [22] T. Nakagawa, T. Matsushima, S. Kawano, Y. Nakazawa, Y. Kato, Y. Adachi, T. Abe, T. Semba, A. Yokoi, J. Matsui, A. Tsuruoka, Y. Funahashi, Lenvatinib in combination with golvatinib overcomes hepatocyte growth factor pathway-induced resistance to vascular endothelial growth factor receptor inhibitor, *Cancer Sci.* 105(6) (2014) 723-730.
- [23] P. Marks, R.A. Rifkind, V.M. Richon, R. Breslow, T. Miller, W.K. Kelly, Histone deacetylases and cancer: causes and therapies, *Nat. Rev. Cancer* 1 (2001) 194-202.
- [24] J.E. Bolden, M.J. Peart, R.W. Johnstone, Anticancer activities of histone deacetylase inhibitors, *Nat. Rev. Drug Discov.* 5 (2006) 769-784.
- [25] P.A. Marks, W.-S. Xu, Histone Deacetylase Inhibitors: Potential in Cancer Therapy, *J. Cell. Biochem.* 107 (2009) 600-608.
- [26] S.B. Baylin, J.E. Ohm, Epigenetic gene silencing in cancer- a mechanism for early oncogenic pathway addiction? *Nat. Rev. Cancer* 6 (2006) 107-116.
- [27] M. Paris, M. Porcelloni, M. Binaschi, D. Fattori, Histone Deacetylase Inhibitors: From Bench to Clinic, *J. Med. Chem.* 51 (6) (2008) 1505-1529
- [28] P. Bertrand, Inside HDAC with HDAC inhibitors, *Eur. J. Med. Chem.* 45 (2010) 2095-2116.
- [29] Q.H. Sodji, V. Patil, J.R. Kornacki, M. Mrksich, A.K. Oyelere, Synthesis and structure-activity relationship of 3-hydroxypyridine-2-thione-based histone deacetylase inhibitors, *J. Med. Chem.* 56 (2013) 9969-9981.
- [30] Y. Yao, C. Liao, Z. Li, Z. Wang, Q. Sun, C. Liu, Y. Yang, Z. Tu, S. Jiang, Design, synthesis, and biological evaluation of 1, 3-disubstituted-pyrazole derivatives as new class I and IIb histone deacetylase inhibitors, *Eur. J. Med. Chem.* 86 (2014) 639-652.
- [31] R. Cincinelli, L. Musso, G. Giannini, V. Zuco, M. De Cesare, F. Zunino, S. Dallavalle, Influence of the adamantyl moiety on the activity of biphenylacrylohydroxamic acid-based HDAC inhibitors, *Eur. J. Med. Chem.* 79 (2014) 251-259.

- [32] Q. Tan, Z. Zhang, J. Hui, Y. Zhao, L. Zhu, Synthesis and anticancer activities of thieno[3,2-d]pyrimidines as novel HDAC inhibitors, *Bioorg. Med. Chem.* 22 (2014) 358-365.
- [33] J. Cai, H. Wei, K.H. Hong, X. Wu, M. Cao, X. Zong, L. Li, C. Sun, J. Chen, M. Ji, Discovery and preliminary evaluation of 2-aminobenzamide and hydroxamate derivatives containing 1,2,4-oxadiazole moiety as potent histone deacetylase inhibitors, *Eur. J. Med. Chem.* 96 (2015) 1-13.
- [34] X. Li, J. Hou, X. Li, Y. Jiang, X. Liu, W. Mu, Y. Jin, Y. Zhang, W. Xu, Development of 3-hydroxycinnamamide-based HDAC inhibitors with potent in vitro and in vivo anti-tumor activity, *Eur. J. Med. Chem.* 89 (2015) 628-637.
- [35] K.T. Thurn, S. Thomas, A. Moore, P.N. Munster, Rational therapeutic combinations with histone deacetylase inhibitors for the treatment of cancer, *Future Oncol.* 7(2) 2011 263-283.
- [36] M.J. Kim, D.E. Kim, I.G. Jeong, J. Choi, S. Jang, J.H. Lee, S. Ro, J.J. Hwang, C.S. Kim, HDAC inhibitors synergize antiproliferative effect of sorafenib in renal cell carcinoma cells, *Anticancer Res.* 32(8) 2012 3161-3168.
- [37] M. Bots, R.W. Johnstone, Rational Combinations Using HDAC Inhibitors, 15 2009 3970-3977.
- [38] T. Nakagawa, S. Takeuchi, T. Yamada, H. Ebi, T. Sano, S. Nanjo, D. Ishikawa, M. Sato, Y. Hasegawa, Y. Sekido, S. Yano, EGFR-TKI resistance due to BIM polymorphism can be circumvented in combination with HDAC inhibition, *Cancer Res.* 73(8) (2013) 2428-2434.
- [39] M.C. Chen, C.H. Chen, J.C. Wang, A.C. Tsai, J.P. Liou, S.L. Pan, C.M. Teng, The HDAC inhibitor, MPT0E028, enhances erlotinib-induced cell death in EGFR-TKI-resistant NSCLC cells, *Cell Death Dis.* 4 (2013) e810.
- [40] X. Cai, H.-X. Zhai, J. Wang, J. Forrester, H. Qu, L. Yin, C.-J. Lai, R. Bao, C. Qian, Discovery of 7-(4-(3-Ethynylphenylamino)-7-methoxyquinazolin-6-yloxy)-N-hydroxyheptanamide (CUDC-101) as a Potent Multi-Acting HDAC, EGFR, and HER2 Inhibitor for the Treatment of Cancer, *J. Med. Chem.* 53 (2010) 2000-2009.
- [41] S. Mahboobi, A. Sellmer, M. Winkler, E. Eichhorn, H. Pongratz, T. Ciossek, T. Baer, T. Maier, T. Beckers, Novel chimeric histone deacetylase inhibitors: a series of lapatinib hybrides as potent inhibitors of epidermal growth factor receptor (EGFR), human epidermal growth factor receptor 2 (HER2), and histone deacetylase activity. *J.*

- Med. Chem. 53(24) (2010) 8546-8555.
- [42] A. Uecker, M. Sicker, T. Beckers, S. Mahboobi, D. Hägerstrand, A. Ostman, F.D. Böhmer, Chimeric tyrosine kinase-HDAC inhibitors as antiproliferative agents, *Anti-cancer Drug.* 21(8) (2010) 759-65.
- [43] T. Beckers, S. Mahboobi, A. Sellmer, M. Winkler, E. Eichhorn, H. Pongratz, T. Maier, T. Ciossek, T. Baer, G. Kelter, H.-H. Fiebig, M. Schmidt, Chimerically designed HDAC- and tyrosine kinase inhibitors. A series of erlotinib hybrids as dual-selective inhibitors of EGFR, HER2 and histone deacetylases, *Med. Chem. Commun.* 3 (2012) 829-835.
- [44] C.-Q. Ning, C. Lu, L. Hu, Y.-J. Bi, L. Yao, Y.-J. He, L.-F. Liu, X.-Y. Liu, N.-F. Yu, Macrocyclic compounds as anti-cancer agents: Design and synthesis of multi-acting inhibitors against HDAC, FLT3 and JAK2, *Eur. J. Med. Chem.* 95 (2015) 104-115.
- [45] H. Patel, I. Chuckowree, P. Coxhead, M. Guille, M. Wang, A. Zuckermann, R. S. B. Williams, M. Librizzi, R. M. Paranal, J. E. Bradner, J. Spencer, Synthesis of hybrid anticancer agents based on kinase and histone deacetylase inhibitors, *Med. Chem. Commun.* 5 (2014) 1829-1833.
- [46] M.H. Potashman, J. Bready, A. Coxon, T.M. Demelfi, L. Dipietro, N. Doerr, D. Elbaum, J. Estrada, P. Gallant, J. Germain, Y. Gu, J.C. Harmange, S.A. Kaufman, R. Kendall, J.L. Kim, G.N. Kumar, A.M. Long, S. Neervannan, V.F. Patel, A. Polverino, P. Rose, S.V. Plas, D. Whittington, R. Zanon, H. Zhao, Design, synthesis, and evaluation of orally active benzimidazoles and benzoxazoles as vascularendothelial growth factor-2 receptor tyrosine kinase inhibitors, *J. Med. Chem.* 50 (2007) 4351-4373.
- [47] M.S. Finnin, J.R. Donigian, A. Cohen, V.M. Richon, R.A. Rifkind, P.A. Marks, R. Breslow, N.P. Pavletich, Structures of a histone deacetylase homologue bound to the TSA and SAHA inhibitors, *Nature* 401 (1999) 188-193.
- [48] L. Shi, T.-T. Wu, Z. Wang, J.-Y. Xue, Y.-G. Xu, Discovery of N-(2-phenyl-1H-benzo[d]imidazol-5-yl)quinolin-4-amine derivatives as novel VEGFR-2 kinase inhibitors, *Eur. J. Med. Chem.* 84 (2014) 698-707.

Captions:

Table 1. VEGFR-2 and HDAC inhibitory activities and antiproliferative activities against MCF-7 of target *N*-phenylquinazolin-4-amine hybrids.

Table 2. HDAC isoenzymes inhibitory activities of compound **6fd**.

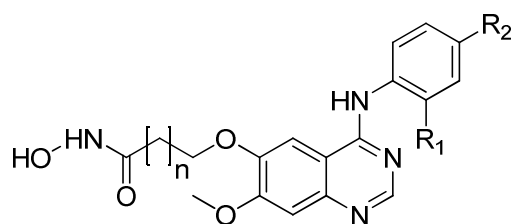
Figure 1. Design of dual inhibitors against VEGFR-2 and HDAC.

Figure 2. (A) 2D molecular docking modeling of compound **6fd** with VEGFR-2. The hydrogen bonds are displayed as green or blue dotted lines. The π -cation interactions are shown as yellow line. (B) 3D model of the interaction between compound **6fd** and VEGFR-2 kinase ATP binding site.

Figure 3. (A) 2D molecular docking modeling of compound **6fd** with HDLP. The hydrogen bonds are displayed as green or blue dotted lines. (B) 3D model of the interaction between compound **6fd** and the active site of HDLP.

Scheme 1. General procedure for the synthesis of *N*-phenylquinazolin-4-amine hybrids. Reagents and conditions: (a) SOCl₂, DMF, reflux; (b) substituted aniline, isopropanol, reflux; (c) LiOH·H₂O, CH₃OH, H₂O; (d) ethyl bromoalkanoate, K₂CO₃, DMF, 40°C; (e) NH₂OH, CH₃OH, 0 °C to rt.

Table 1



No.	Compound			VEGFR-2	HDAC	MCF-7
	R ₁	R ₂	n	(IC ₅₀ , nM)	(IC ₅₀ , nM)	(IC ₅₀ , μM)
6aa	F	H	2	865	673	>100
6ab	F	H	3	840	554	>100
6ac	F	H	4	918	145	84
6ad	F	H	5	754	32	15
6ba	H	F	2	376	1340	>100
6bb	H	F	3	455	139	74
6bc	H	F	4	524	29	18
6bd	H	F	5	270	8.5	2.4
6ca	Cl	H	2	857	1255	>100
6cb	Cl	H	3	832	128	78
6cc	Cl	H	4	685	29	15
6cd	Cl	H	5	364	18	7.8
6da	H	Cl	2	182	698	85
6db	H	Cl	3	220	132	61
6dc	H	Cl	4	313	11	4.0
6dd	H	Cl	5	215	3.2	1.7
6ea	Br	H	2	>10000	840	>100
6eb	Br	H	3	>10000	74	33
6ec	Br	H	4	>10000	31	17
6ed	Br	H	5	>10000	8.8	2.6
6fa	H	Br	2	98	545	52
6fb	H	Br	3	59	68	36

6fc	H	Br	4	153	12	3.5
6fd	H	Br	5	74	2.2	0.85
Vandetanib				54	>10000	18.5
Vorinostat				>10000	15	4.2

Table 2

HDAC isoenzyme	IC ₅₀ (nM)
HDAC1	1.8
HDAC2	3.3
HDAC6	16.4
HDAC8	4.6

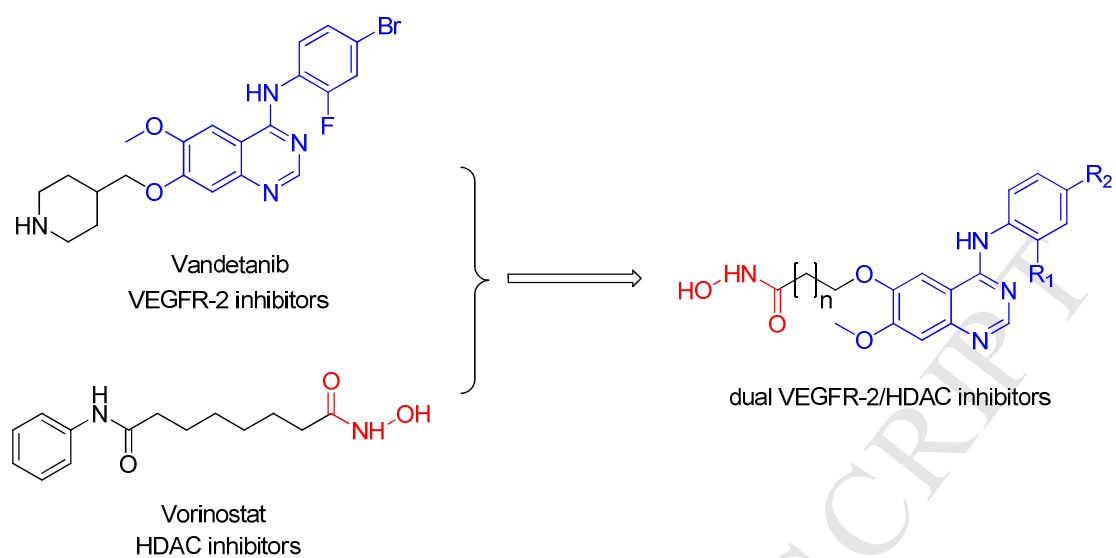


Figure 1

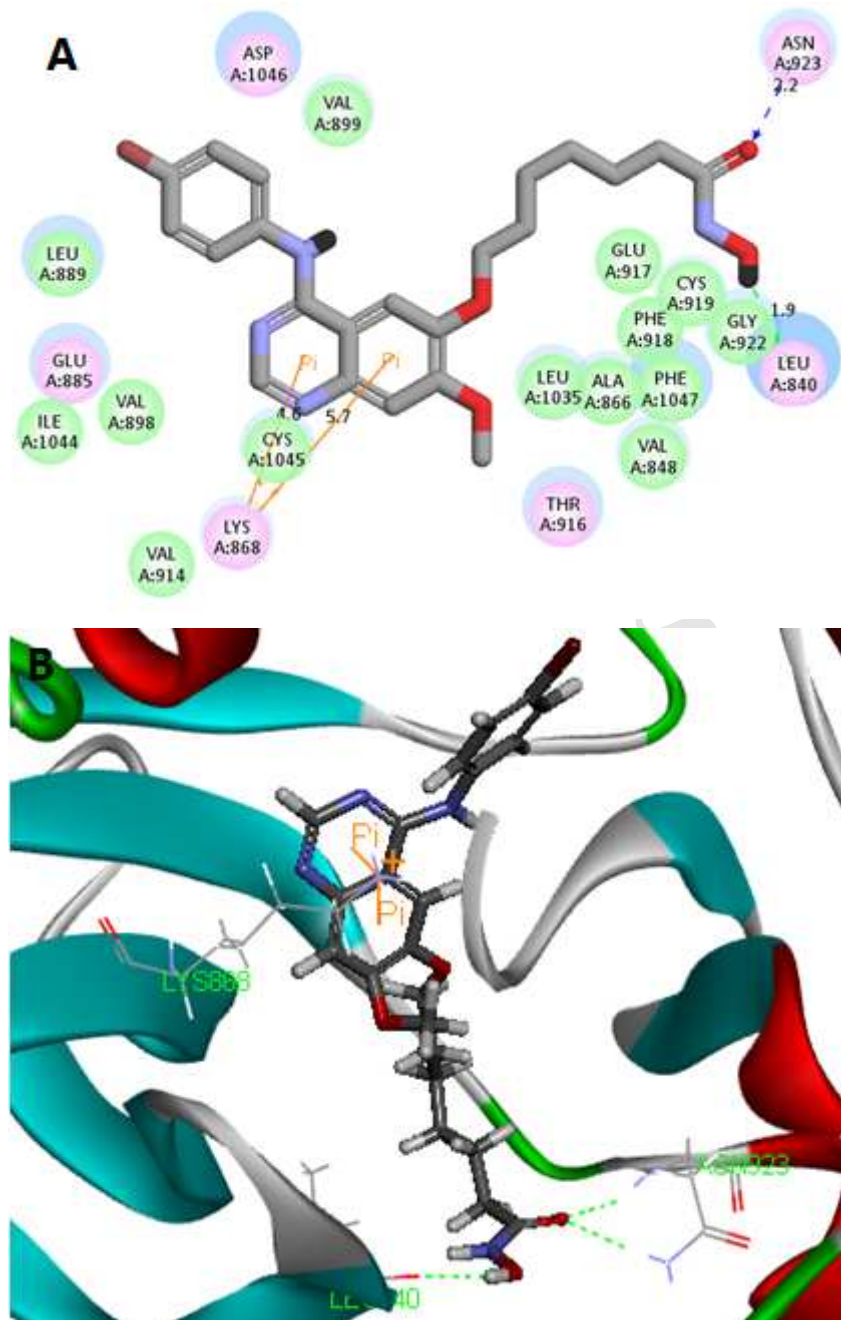


Figure 2

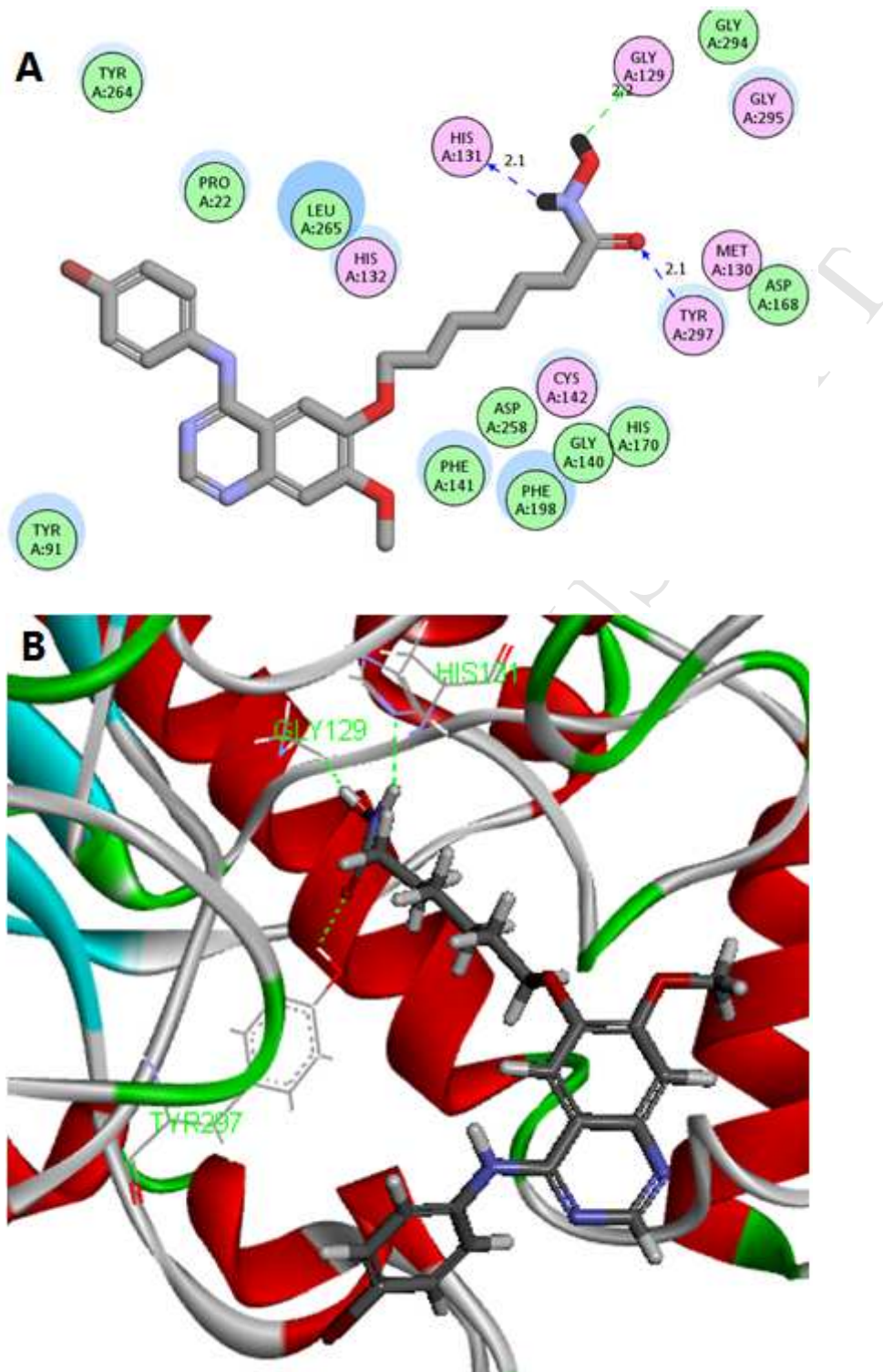
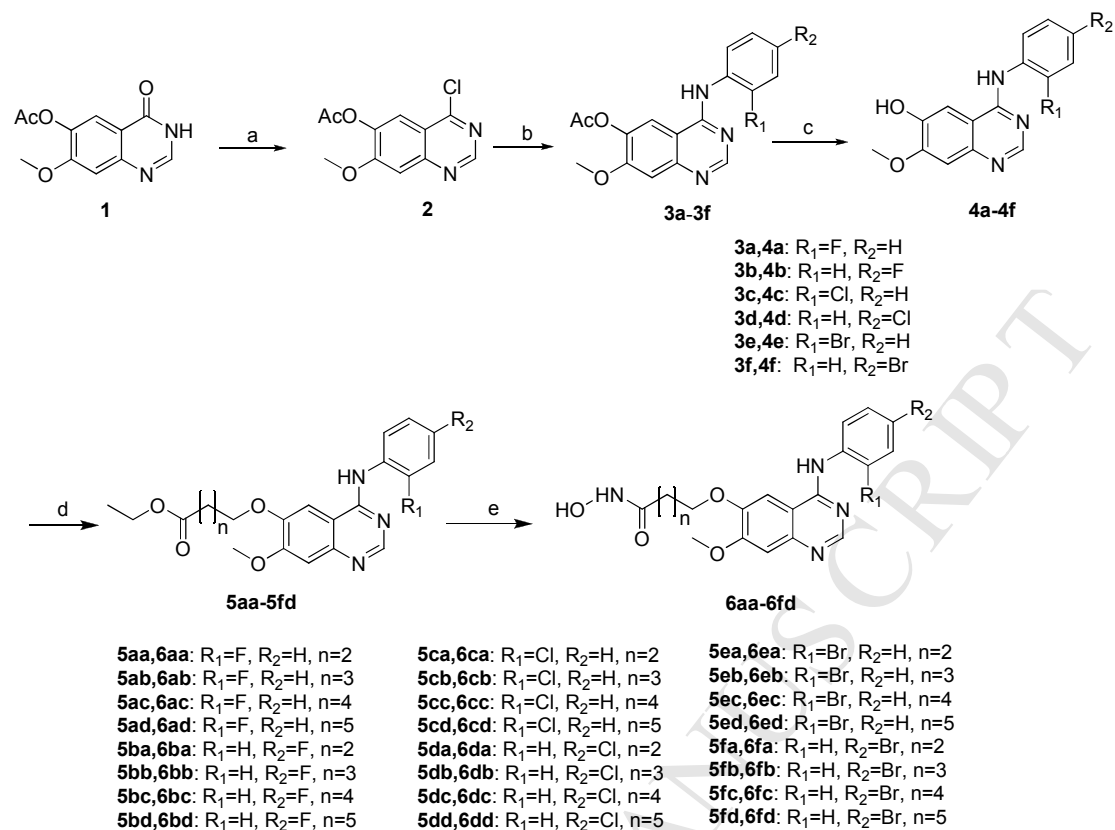


Figure 3



Scheme 1

- 24 Novel hybrids were synthesized as dual VEGFR-2/HADC inhibitors.
- The *in vitro* enzymatic and cellular activities were evaluated.
- The primary structure-activity relationships were discussed.
- Compound **6fd** exhibited the most potent biological activities.